
Hyperparameter Tuning is All You Need for LISTA

Xiaohan Chen^{1*} Jialin Liu^{2*} Zhangyang Wang¹ Wotao Yin²

¹University of Texas at Austin ²Alibaba US, Damo Academy
 {xiaohan.chen, atlaswang}@utexas.edu
 {jialin.liu, wotao.yin}@alibaba-inc.com

Abstract

Learned Iterative Shrinkage-Thresholding Algorithm (LISTA) introduces the concept of unrolling an iterative algorithm and training it like a neural network. It has had great success on sparse recovery. In this paper, we show that adding momentum to intermediate variables in the LISTA network achieves a better convergence rate and, in particular, the network with instance-optimal parameters is superlinearly convergent. Moreover, our new theoretical results lead to a practical approach of automatically and adaptively calculating the parameters of a LISTA network layer based on its previous layers. Perhaps most surprisingly, such an adaptive-parameter procedure reduces the training of LISTA to tuning **only three hyperparameters** from data: a new record set in the context of the recent advances on trimming down LISTA complexity. We call this new ultra-light weight network *HyperLISTA*. Compared to state-of-the-art LISTA models, HyperLISTA achieves almost the same performance on seen data distributions and performs better when tested on unseen distributions (specifically, those with different sparsity levels and nonzero magnitudes). Code is available: <https://github.com/VITA-Group/HyperLISTA>.

1 Introduction

In this paper, we study the sparse linear inverse problem, where we strive to recover an unknown sparse vector $\mathbf{x}^* \in \mathbb{R}^n$ from its noisy linear measurement \mathbf{b} generated from

$$\mathbf{b} = \mathbf{A}\mathbf{x}^* + \varepsilon, \quad (1)$$

where $\mathbf{b} \in \mathbb{R}^m$ is the measurement that we observe, $\mathbf{A} \in \mathbb{R}^{m \times n}$ is the *dictionary*, $\mathbf{x}^* \in \mathbb{R}^n$ is the unknown ground truth that we aim to recover, and $\varepsilon \in \mathbb{R}^m$ is additive Gaussian white noise. For simplicity, each column of \mathbf{A} , is normalized to have unit ℓ_2 norm. Typically, we have much fewer rows than columns in the dictionary \mathbf{A} , i.e., $m \ll n$. Therefore, Equation (1) is an under-determined system. The sparse inverse problem, also known as sparse coding, plays essential roles in a wide range of applications including feature selection, signal reconstruction and pattern recognition.

Sparse linear inverse problems are well studied in the literature of optimization. For example, it can be formulated into LASSO [29] and solved by many optimization algorithms [9, 3]. These solutions explicitly consider and incorporate the sparsity prior and usually exploit iterative routines. Deep-learning-based approaches are proposed for empirically solving inverse problems recently [25], which produce black-box models that are trained with data in an end-to-end way, while somehow ignoring the sparsity prior. Comparing the two streams, the former type, i.e., the classic optimization methods, takes hundreds to thousands of iterations to generate accurate solutions, while black-box deep learning models, if properly trained, can achieve similar accuracy in tens of layers. However, classic methods come with data-agnostic convergence (rate) guarantees under suitable conditions,

*The first two authors made equal contributions.

whereas deep learning methods only empirically work for instances similar to the training data, lacking theoretical guarantees and interpretability. More discussions are found in [6].

Unrolling is an uprising approach that bridges the two streams [22, 21]. By converting each iteration of a classic iterative algorithm into one layer of a neural network, one can *unroll* and truncate a classic optimization method into a feed-forward neural network, with a finite number of layers. Relevant parameters (e.g., the dictionary, step sizes and thresholds) in the original algorithm are transformed into learnable weights, that are trained on data. [15] pioneered the unrolling scheme for solving sparse coding and achieved great empirical success. By unrolling the Iterative Shrinkage-Thresholding Algorithm (ISTA), the authors empirically demonstrated up to two magnitudes of acceleration of the learned ISTA (LISTA) compared to the original ISTA. The similar unrolling idea was later extended to numerous optimization problems and algorithms [28, 30, 26, 13, 36, 2, 16, 8, 5].

1.1 Related Works

The balance between empirical performance and interpretability of unrolling motivates a line of theoretical efforts to explain their acceleration success. [23] attempted to understand LISTA by re-factorizing the Gram matrix of the dictionary \mathbf{A} in (1) and proved that such re-parameterization converges sublinearly and empirically showed that it achieved similar acceleration gain to LISTA. [33] investigated unrolling iterative hard thresholding (IHT) and proved the existence of a matrix transformation that can improve the restricted isometry property constant of the original dictionary. Although it is difficult to search for the optimal transformation using classic optimization techniques, the authors of [33] argued that the data-driven training process is able to learn that transformation from data, and hence achieving the acceleration effect in practice.

The work [7] extended the weight coupling necessary condition in [33] to LISTA. The authors for the first time proved the existence of a learnable parameter set that guarantees linear convergence of LISTA. Later in [18], they further showed that the weight matrix in [7] can be analytically derived from the dictionary \mathbf{A} and free from learning, reducing the learnable parameter set to only tens of scalars (layer-wise step sizes and thresholds). The resulting algorithm, called Analytic LISTA (ALISTA), sets one milestone in simplifying LISTA. [31] extends ALISTA by introducing gain and overshoot gating mechanisms and integrate them into unrolling. [37] proposed error-based thresholding (EBT), which leverages a function of the layer-wise reconstruction error to suggest an appropriate threshold value for each observation on each layer. Another interesting work [4] uses a black-box LSTM model that takes the historical residual and update quantity as input and generates layerwise step sizes and thresholds in ALISTA. Their proposed model, called Neurally Augmented ALISTA (NA-ALISTA), performed well in large-scale problems.

1.2 Our Contributions

Our research question is along the line of [18, 37, 4]: *can we improve the LISTA parameterization, by further disentangling the learnable parameters from the observable terms (e.g., reconstruction errors, intermediate outputs)?* Our aim is to create more light-weight, albeit more robust LISTA models with “baked in” adaptivity to testing samples from unseen distributions. The goal should be achieved without sacrificing our previously attained benefits: empirical performance, and convergence (rate) guarantees – if not improving them further.

We present an affirmative answer to the above question by learning instance-optimal parameters with a new ALISTA parameterization. First, we prove that by augmenting ALISTA with momentum, the new unrolled network can achieve a better convergence rate over ALISTA. Second, we find that once the above LISTA network is further enabled with instance-optimal parameters, then a superlinear convergence can be attained. Lastly, we show that those instance-optimal parameters of each layer can be generated in closed forms, consequently reducing ALISTA to only learning **three instance- and layer-invariant hyperparameters**.

Our new ultra-light weight network is termed as *HyperLISTA*. Compared to ALISTA, the new parameterization of HyperLISTA facilitates new backpropagation-free “training” options (e.g., bayesian optimization), and can unroll to more iterations in testing than training thanks to its layer-wise decomposed form. When comparing to state-of-the-art LISTA variants in experiments, HyperLISTA achieves the same strong performance on seen data distributions, and performs better when tested on unseen distributions (e.g., with different sparsity levels and nonzero magnitudes). In the supple-

mentary materials, we also show that the superlinear convergence can be observed in HyperLISTA experiments, when our automatic parameter tuning is performed per instance.

2 Assumptions and Preliminaries

Mathematical Notations: We represent a matrix as a capital bold letter \mathbf{W} , $\text{diag}(\mathbf{W})$ means the diagonal elements of matrix \mathbf{W} and the pseudoinverse of a matrix is denoted by \mathbf{W}^+ . A vector is represented as a lowercase bold letter \mathbf{x} and its entries are represented as lowercase regular letters with lower indices $\mathbf{x} = [x_1, x_2, \dots, x_3]^T$. Upper indices represent iterations or layers. Moreover, $\mathbf{0}$, $\mathbf{1}$ represent a vector with all zeros or all ones, respectively. “ $\text{supp}(\mathbf{x})$ ” denotes the support, the indices of all nonzeros in vector \mathbf{x} .

ISTA Algorithm: With an ℓ_1 penalty term, the minimizer of LASSO, $\text{argmin}_{\mathbf{x}} \frac{1}{2} \|\mathbf{A}\mathbf{x} - \mathbf{b}\|_2^2 + \lambda \|\mathbf{x}\|_1$, provides an estimate of the solution of the sparse recovery problem (1). A popular algorithm to solve LASSO is Iterative Shrinkage-Thresholding Algorithm (ISTA):

$$\mathbf{x}^{(k+1)} = \eta_{\lambda/L} \left(\mathbf{x}^{(k)} + \frac{1}{L} \mathbf{A}^T (\mathbf{b} - \mathbf{A}\mathbf{x}^{(k)}) \right), \quad k = 0, 1, 2, \dots$$

where $\eta_{\lambda/L}$ is the element-wise soft-thresholding function $\eta_{\theta}(\mathbf{x}) = \text{sign}(\mathbf{x}) \max(0, |\mathbf{x}| - \theta)$ with $\theta = \lambda/L$ and L is usually taken as the largest eigenvalue of $\mathbf{A}^T \mathbf{A}$.

LISTA Model: The original LISTA work [15] parameterizes ISTA as

$$\mathbf{x}^{(k+1)} = \eta_{\theta^{(k)}} \left(\mathbf{W}_1^{(k)} \mathbf{x}^{(k)} + \mathbf{W}_2^{(k)} \mathbf{b} \right), \quad k = 0, 1, 2, \dots \quad (2)$$

where $\Theta = \{\mathbf{W}_1^{(k)}, \mathbf{W}_2^{(k)}, \theta^{(k)}\}$ are learnable parameters to train from data. In the training process, iterations formulated in (2) are unrolled and truncated to K steps and the parameters are trained by minimizing the following loss function defined over the distribution of training samples D_{tr} :

$$\text{minimize}_{\Theta} \mathbb{E}_{(\mathbf{x}^*, \mathbf{b}) \sim D_{\text{tr}}} \left\| \mathbf{x}^{(K)}(\Theta, \mathbf{b}, \mathbf{x}^{(0)}) - \mathbf{x}^* \right\|_2^2. \quad (3)$$

Here $\mathbf{x}^{(K)}(\Theta, \mathbf{b}, \mathbf{x}^{(0)})$, the output of the LISTA model, is a function with input Θ , \mathbf{b} and $\mathbf{x}^{(0)}$. In practice, we usually set $\mathbf{x}^{(0)} = \mathbf{0}$. We will use $\mathbf{x}^{(K)}$ to refer to $\mathbf{x}^{(K)}(\Theta, \mathbf{b}, \mathbf{x}^{(0)})$ for brevity in the remainder of this paper. \mathbf{x}^* denotes the underlying ground truth defined in (1). Although it cannot be accessed in iterative algorithm (2), it can be used as the label in supervised training (3).

ALISTA Model: ALISTA [18] advances LISTA with a lighter and more interpretable parameterization, where the learnable parameters are $\Theta = \{\gamma^{(k)}, \theta^{(k)}\}$ and the iterations are formulated as

$$\mathbf{x}^{(k+1)} = \eta_{\theta^{(k)}}^{p^{(k)}} \left(\mathbf{x}^{(k)} + \gamma^{(k)} \mathbf{W}^T (\mathbf{b} - \mathbf{A}\mathbf{x}^{(k)}) \right), \quad (4)$$

where \mathbf{W} is calculated by solving the following optimization problem:

$$\mathbf{W} \in \underset{\mathbf{W} \in \mathbb{R}^{m \times n}}{\text{argmin}} \left\| \mathbf{W}^T \mathbf{A} \right\|_F^2, \quad \text{s.t. } \text{diag}(\mathbf{W}^T \mathbf{A}) = \mathbf{1}. \quad (5)$$

The thresholding operator is improved with support selection. At layer k , a certain percentage of entries with largest magnitudes are trusted as “true support” and will not be passed through thresholding. Specifically, the i -th element of $\eta_{\theta^{(k)}}^{p^{(k)}}(\mathbf{v})$ is defined as

$$\left(\eta_{\theta^{(k)}}^{p^{(k)}}(\mathbf{v}) \right)_i = \begin{cases} v_i & : v_i > \theta^{(k)}, & i \in S^{p^{(k)}}(\mathbf{v}), \\ v_i - \theta^{(k)} & : v_i > \theta^{(k)}, & i \notin S^{p^{(k)}}(\mathbf{v}), \\ 0 & : -\theta^{(k)} \leq v_i \leq \theta^{(k)} \\ v_i + \theta^{(k)} & : v_i < -\theta^{(k)}, & i \notin S^{p^{(k)}}(\mathbf{v}), \\ v_i & : v_i < -\theta^{(k)}, & i \in S^{p^{(k)}}(\mathbf{v}), \end{cases} \quad (6)$$

where $S^{p^{(k)}}(\mathbf{v})$ includes the elements with the largest $p^{(k)}$ magnitudes in vector $\mathbf{v} \in \mathbb{R}^n$:

$$S^{p^{(k)}}(\mathbf{v}) = \left\{ i_1, i_2, \dots, i_{p^{(k)}} \mid |v_{i_1}| \geq |v_{i_2}| \geq \dots \geq |v_{i_{p^{(k)}}}| \geq |v_{i_n}| \right\}. \quad (7)$$

With $p^{(k)} = 0$, the operator reduces to the soft-thresholding and, with $p^{(k)} = n$, the operator reduces to the hard-thresholding. Thus, operator $\eta_{\theta^{(k)}}^{p^{(k)}}(\mathbf{v})$ is actually a balance between soft- and hard-thresholding. When k is small, $p^{(k)}$ is usually chosen as a small fraction of n and the operator tends to not trust the signal, and vice versa. In ALISTA, $p^{(k)}$ is proportional to the index k , capped by a maximal value, i.e., $p^{(k)} = \min(p \cdot k, p_{\max})$, where p and p_{\max} are two hyperparameters that will be tuned manually. Later in this work, we will consider $p^{(k)}$ as a parameter that could be adaptively calculated by the information from previous iterations (layers).

More Notations and Assumptions: Throughout this paper, we refer to “parameters” as the learnable weights in the models, such as the thresholds $\theta^{(k)}$ and the step sizes $\gamma^{(k)}$ that are defined in the ALISTA model, which are usually trained by back-propagation. In contrast, we refer “hyperparameters” as those constants that are often ad-hoc pre-defined to calculate parameters. For example, $\theta^{(k)} = c_1 \|\mathbf{A}^+(\mathbf{A}\mathbf{x}^{(k)} - \mathbf{b})\|_1$, where $\theta^{(k)}$ is a parameter and c_1 is a hyperparameter.

Assumption 1 (Basic assumptions). *The signal \mathbf{x}^* and noise ε are sampled from the following set:*

$$\mathcal{X}(B, \underline{B}, s, \sigma) \triangleq \left\{ (\mathbf{x}^*, \varepsilon) \mid \|\varepsilon\|_1 \leq \sigma, \|\mathbf{x}^*\|_0 \leq s, 0 < \underline{B} \leq |\mathbf{x}_i^*| \leq B, \forall i \in \text{supp}(\mathbf{x}^*) \right\}. \quad (8)$$

In other words, \mathbf{x}^* is bounded and sparse. $\sigma > 0$ is the noise level.

Compared with the Assumption 2 in [7], the assumption of “ $|\mathbf{x}_i^*| \geq \underline{B} > 0$ ” for non-zero elements in \mathbf{x}^* is slightly stronger. But we will justify (after Theorem 1) that uniformly under Assumption 1 in this paper, our method also achieves a better convergence rate than state-of-the-arts.

3 Methodologies and Theories

In this section, we extend the ALISTA (4) in three aspects. First, we introduce a better method to calculate matrix \mathbf{W} in formula (5). Second, we augment the x-update formula (4) by adding a momentum term. Finally, we propose an adaptive approach to obtain the parameters $p^{(k)}, \theta^{(k)}, \gamma^{(k)}$.

3.1 Preparation: Symmetric Jacobian of Gradients

Before improving the formula (5), we first briefly explain its main concepts and shortcomings. Mutual coherence is a key concept in compressive sensing[11, 10]. For matrix \mathbf{A} , it is defined as $\max_{i \neq j} |(\mathbf{A}^T \mathbf{A})_{i,j}|$ where $(\mathbf{A}^T \mathbf{A})_{i,i} = 1$ since each column of \mathbf{A} is assumed with unit ℓ_2 norm. A matrix with low mutual coherence satisfies that $\mathbf{A}^T \mathbf{A}$ approximates the identity matrix, thus implying a recovery of high probability. In ALISTA [18], the authors extended this concept to a relaxed bound between matrix \mathbf{A} and another matrix \mathbf{W} : $\|\mathbf{W}^T \mathbf{A}\|_F$ (described in (5)). By minimizing this bound, they obtained a good matrix \mathbf{W} that can be plugged into the LISTA framework.

One clear limitation of ALISTA is that, with \mathbf{W} obtained by (5), the model is only able to converge to \mathbf{x}^* but not the LASSO minimizer [2]. Consequently, one has to train ALISTA with known \mathbf{x}^* in a supervised way (3). This is partially due to the fact that the update direction $\mathbf{W}^T(\mathbf{A}\mathbf{x} - \mathbf{b})$ in ALISTA is not aligned with the gradient of the ℓ_2 term in the LASSO objective: $\nabla_{\mathbf{x}} \frac{1}{2} \|\mathbf{A}\mathbf{x} - \mathbf{b}\|_2^2 = \mathbf{A}^T(\mathbf{A}\mathbf{x} - \mathbf{b})$. This limitation motivates us to adopt a new symmetric Jacobian parameterization so that $\mathbf{W}^T \mathbf{A}$ is symmetric and the coherence between \mathbf{A} and \mathbf{W} is minimized.

Inspired by [1], we define $\mathbf{W} = (\mathbf{G}^T \mathbf{G})\mathbf{A}$ (the matrix $\mathbf{G} \in \mathbb{R}^{m \times m}$ is named as the Gram matrix), and get the following problem instead of (5):

$$\min_{\mathbf{G}} \|\mathbf{A}^T \mathbf{G}^T \mathbf{G} \mathbf{A} - \mathbf{I}\|_F^2, \quad \text{s.t. } \text{diag}(\mathbf{A}^T \mathbf{G}^T \mathbf{G} \mathbf{A}) = \mathbf{1}. \quad (9)$$

However, the constraint in the above problem (9) is hard to handle. Thus, we introduce an extra matrix $\mathbf{D} = \mathbf{G}\mathbf{A} \in \mathbb{R}^{m \times n}$ and use the following method instead to calculate dictionary:

$$\min_{\mathbf{G}, \mathbf{D}} \|\mathbf{D}^T \mathbf{D} - \mathbf{I}\|_F^2 + \frac{1}{\alpha} \|\mathbf{D} - \mathbf{G}\mathbf{A}\|_F^2, \quad \text{s.t. } \text{diag}(\mathbf{D}^T \mathbf{D}) = \mathbf{1}. \quad (10)$$

With proper $\alpha > 0$, the solution of (10) approximates (9) well. We use an adaptive rule to choose α and adopt a variant of the algorithm (described in details in the supplement) proposed in [19] to solve (10). Such formula leads to a symmetric matrix $\mathbf{W}^T \mathbf{A} = (\mathbf{G}\mathbf{A})^T (\mathbf{G}\mathbf{A})$. With this symmetry, the vector $\mathbf{W}^T(\mathbf{A}\mathbf{x} - \mathbf{b})$ is actually the gradient of function $\frac{1}{2} \|\mathbf{G}(\mathbf{A}\mathbf{x} - \mathbf{b})\|_2^2$ with respect to \mathbf{x} .

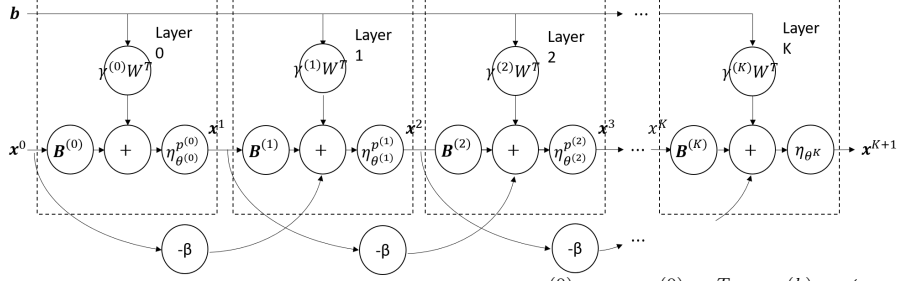


Figure 1: ALISTA with momentum as formulated in (12), with $\mathbf{B}^{(0)} = \mathbf{I} - \gamma^{(0)} \mathbf{W}^T \mathbf{A}$, $\mathbf{B}^{(k)} = (1 + \beta^{(k)}) \mathbf{I} - \gamma^{(k)} \mathbf{W}^T \mathbf{A}$ ($k \geq 1$). The momentum creates extra skip connections at the bottom.

One may train model (4) using methods in [2] with the following loss function without knowing the ground truth: $F(\mathbf{x}) = \frac{1}{2} \|\mathbf{G}(\mathbf{A}\mathbf{x} - \mathbf{b})\|_2^2 + \lambda \|\mathbf{x}\|_1$. On the other hand, it usually holds that

$$\|\mathbf{W}^T \mathbf{A} - \mathbf{I}\|_F \approx \|(\mathbf{G}\mathbf{A})^T (\mathbf{G}\mathbf{A}) - \mathbf{I}\|_F, \quad (11)$$

where \mathbf{W} is calculated by (5) and \mathbf{G} is calculated by (10). We validate (11) by numerical results in Section 4.1. Conclusion (11) demonstrates that the mutual coherence between \mathbf{A} and $(\mathbf{G}^T \mathbf{G})\mathbf{A}$ is similar to that between \mathbf{A} and \mathbf{W} obtained by (5). Although we limit the matrix $\mathbf{W}^T \mathbf{A}$ to be symmetric, (10) hardly degrades any performance of the ALISTA framework compared to (5).

3.2 ALISTA with Momentum: Improved Linear Convergence Rate

As is well known in the optimization community, adding a momentum term can accelerate many iterative algorithms. Two classic momentum algorithms were respectively proposed by Polyak [27] and Nesterov [24]. Nesterov's algorithm alternates between the gradient update and the extrapolation, while Polyak's algorithm can be written as an iterative algorithm within the space of gradient updates by simply adding a momentum term. To avoid extra training overhead, we use Polyak's heavy ball scheme and add a momentum term to the ALISTA formula for $k \geq 1$ ² (illustrated in Figure 1):

$$\mathbf{x}^{(k+1)} = \eta_{\theta^{(k)}}^{p^{(k)}} \left(\mathbf{x}^{(k)} + \gamma^{(k)} \mathbf{W}^T (\mathbf{b} - \mathbf{A}\mathbf{x}^{(k)}) + \beta^{(k)} (\mathbf{x}^{(k)} - \mathbf{x}^{(k-1)}) \right) \quad (12)$$

Note that there are other LISTA variants that incorporated additional momentum forms [23, 32], but they did not contribute to provably accelerated convergence rate. Defining constant μ as the mutual coherence of \mathbf{D} , i.e., $\mu := \max_{i \neq j} |(\mathbf{D}_{:,i})^T \mathbf{D}_{:,j}|$, we have the following theorem, which demonstrates that, in the context of (A)LISTA, model (12) can provide a faster linear convergence rate, than that of ALISTA in the same settings.

Theorem 1 (Convergence of ALISTA-Momentum). *Let $\mathbf{x}^{(0)} = \mathbf{0}$ and $\{\mathbf{x}^{(k)}\}_{k=1}^{\infty}$ be generated by (12). If Assumption 1 holds and $s < (1 + 1/\mu)/2$ and σ is small enough, then there exists a uniform sequence of parameter $\{\theta^{(k)}, p^{(k)}, \gamma^{(k)}, \beta^{(k)}\}_{k=1}^{\infty}$ for all $(\mathbf{x}^*, \varepsilon) \in \mathcal{X}(B, \underline{B}, s, \sigma)$ such that*

$$\|\mathbf{x}^{(k)} - \mathbf{x}^*\|_2 \leq C_0 \prod_{t=0}^k c^{(t)} + \frac{2sC_W}{1 - 2\mu s + \mu} \sigma, \quad \forall k = 1, 2, \dots, \quad (13)$$

where $C_0 > 0$ is a constant depending on s, B, μ and $C_W = \max_{1 \leq i, j \leq n} |\mathbf{W}_{i,j}|$. The convergence rate $c^{(k)} > 0$ satisfies:

$$c^{(k)} \leq 2\mu s - \mu < 1, \quad \forall k \quad (14)$$

$$c^{(k)} \leq 1 - \sqrt{1 - 2\mu s + \mu} < 2\mu s - \mu, \quad \forall k \geq \frac{\log(\underline{B}) - \log(2C_0)}{\log(2\mu s - \mu)} \quad (15)$$

and the parameter sequence satisfies

$$\theta^{(k)} = \mu \sup_{(\mathbf{x}^*, \varepsilon) \in \mathcal{X}(B, \underline{B}, s, \sigma)} \left\{ \|\mathbf{x}^{(k)} - \mathbf{x}^*\|_1 + C_W \sigma \right\}, \quad \gamma^{(k)} = 1, \quad \forall k \quad (16)$$

$$\beta^{(k)} \rightarrow (1 - \sqrt{1 - 2\mu s + \mu})^2, \quad p^{(k)} \rightarrow n, \quad \text{as } k \rightarrow \infty$$

²As $k = 0$, we keep the ALISTA formula since $\mathbf{x}^{(-1)}$ is not defined.

Despite remaining linearly convergent, our model has an initial rate of $2\mu s - \mu$ that is no worse than the rates in state-of-the-arts [7, 18, 1] and an eventual rate $1 - \sqrt{1 - 2\mu s + \mu}$ that is strictly better than the rate in [7] because $2\mu s - \mu > 1 - \sqrt{1 - 2\mu s + \mu}$ as $2\mu s - \mu < 1$. For example, if $2\mu s - \mu = 0.9$, then our new rate is $1 - \sqrt{1 - 2\mu s + \mu} \approx 0.684$. Moreover, the eventual error $2sC_W\sigma/(1 - 2\mu s + \mu)$ is no worse than that in [7]. Proof details can be found in the supplement.

3.3 Instance-Adaptive Parameters: From Linear to Superlinear Convergence

State-of-the-art theoretical results show that LISTA converges with a linear rate [7, 18, 1, 31, 35]. In ALISTA [18], the authors show that linear convergence is a lower bound. This means that one cannot expect a superlinear rate if a uniform set of optimal parameters are learned for a dataset.

One promise to enhance the rate in Theorem 1 is to further introduce instance adaptivity. We establish that, if $\{\theta^{(k)}, p^{(k)}, \gamma^{(k)}, \beta^{(k)}\}_{k=1}^{\infty}$ can be searched for an instance, such instance-optimal parameters lead to superlinear convergence.

Theorem 2. *Let $\mathbf{x}^{(0)} = \mathbf{0}$ and $\{\mathbf{x}^{(k)}\}_{k=1}^{\infty}$ be generated by (12). If Assumption 1 holds and $s < (1 + 1/\mu)/2$ and σ is small enough, then there exists a sequence of parameters $\{\theta^{(k)}, p^{(k)}, \gamma^{(k)}, \beta^{(k)}\}_{k=1}^{\infty}$ for each instance $(\mathbf{x}^*, \varepsilon) \in \mathcal{X}(B, \underline{B}, s, \sigma)$ so that we have:*

$$\|\mathbf{x}^{(k)} - \mathbf{x}^*\|_2 \leq \sqrt{sB} \prod_{t=0}^k \bar{c}^{(t)} + \frac{2sC_W}{1 - 2\mu s + \mu} \sigma, \quad \forall k = 1, 2, \dots, \quad (17)$$

where C_W is defined in Theorem 1 and the convergence rate $\bar{c}^{(k)}$ satisfies

$$\bar{c}^{(k)} \rightarrow 0 \text{ as } k \rightarrow \infty. \quad (18)$$

To achieve this super-linear convergence rate, parameters are chosen as follows:

$$\theta^{(k)} = \gamma^{(k)} \left(\mu \|\mathbf{x}^{(k)} - \mathbf{x}^*\|_1 + C_W \sigma \right), \quad \forall k \quad (19)$$

and $p^{(k)}$ follows (16) for all k . The other two parameters $\gamma^{(k)}, \beta^{(k)}$ follow (16) at the initial stage (with small k) and they are instance-adaptive as k large enough. Consequently, the model (12) reduces to the conjugate gradient (CG) iteration on the following linear system as k large enough:

$$\mathbf{W}_S^T (\mathbf{A}_S \mathbf{x}_S - \mathbf{b}) = \mathbf{0}, \quad (20)$$

where S denotes the support of \mathbf{x}^* and $\mathbf{A}_S, \mathbf{W}_S$ denotes, respectively, the sub-matrices of \mathbf{A}, \mathbf{W} with column mask S .

3.4 HyperLISTA: Reducing ALISTA to Tuning Three Hyperparameters

Adaptive Parameters Based on Theorem 2, we design the following instance-adaptive parameter formula as the recovery signal $\mathbf{x}^{(k)}$ is not accurate enough (equivalently, as k is small):

$$\gamma^{(k)} = 1, \quad (21)$$

$$\theta^{(k)} = c_1 \mu \gamma^{(k)} \|\mathbf{A}^+ (\mathbf{A} \mathbf{x}^{(k)} - \mathbf{b})\|_1, \quad (22)$$

$$\beta^{(k)} = c_2 \mu \|\mathbf{x}^{(k)}\|_0, \quad (23)$$

$$p^{(k)} = c_3 \min \left(\log \left(\frac{\|\mathbf{A}^+ \mathbf{b}\|_1}{\|\mathbf{A}^+ (\mathbf{A} \mathbf{x}^{(k)} - \mathbf{b})\|_1} \right), n \right), \quad (24)$$

where $c_1 > 0, c_2 > 0, c_3 > 0$ are hyper-parameters to tune.

The step size formula (21) stems from the conclusion (16) as Theorem 2 suggests. The threshold $\theta^{(k)}$ in (19) cannot be directly used due to its dependency on the ground truth \mathbf{x}^* . In (22), we use $\|\mathbf{A}^+ (\mathbf{A} \mathbf{x}^{(k)} - \mathbf{b})\|_1$ to estimate (19) because

$$\|\mathbf{A}^+ (\mathbf{A} \mathbf{x}^{(k)} - \mathbf{b})\|_1 = \|\mathbf{A}^+ \mathbf{A} (\mathbf{x}^{(k)} - \mathbf{x}^*) - \mathbf{A}^+ \varepsilon\|_1 \approx \mathcal{O}(\|\mathbf{x}^{(k)} - \mathbf{x}^*\|_1) + \mathcal{O}(\sigma).$$

Similar thresholding schemes are studied in [37].

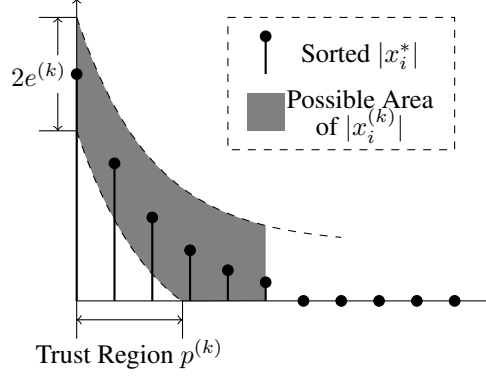


Figure 2: Choice of support selection

The momentum rule (23) is obtained via equation (16). The momentum factor $\beta^{(k)}$ is asymptotically equal to $(1 - \sqrt{1 - 2\mu s + \mu})^2$, which is a monotonic increasing function w.r.t. s , the number of nonzeros in the ground truth sparse vector \mathbf{x}^* . Therefore, ℓ_0 norm of $\mathbf{x}^{(k)}$ is a natural choice to approximate $\beta^{(k)}$, considering that $\mathbf{x}^{(k)}$ will gradually converge to \mathbf{x}^* and hence $\|\mathbf{x}^{(k)}\|_0$ to $\|\mathbf{x}^*\|_0$. The support selection rule (24) can be explained as follows. First we sort the magnitude of $|x_i^*|$ as in Figure 2. At the k -th layer, given $e^{(k)} = \|\mathbf{x}^{(k)} - \mathbf{x}^*\|_\infty$, each element in $\mathbf{x}^{(k)}$ can be bounded as

$$|x_i^*| - e^{(k)} \leq |x_i^{(k)}| \leq |x_i^*| + e^{(k)}, \quad \forall i.$$

Such area is shown as the gray area in Figure 2. As we discussed in Section 2 following definition (6), the support selection is a scheme to select those elements that can be trusted as true support. The ‘‘trust region’’ in Figure 2 illustrates such entries. Intuitively, the trust region should be larger as the error $e^{(k)}$ gets smaller. We propose to use the logarithmic function of the error to estimate $p^{(k)}$.

$$p^{(k)} \approx c_3 \log \left(\frac{\|\mathbf{x}^*\|_\infty}{e^{(k)}} \right) \approx c_3 \log \left(\frac{\|\mathbf{A}^+\mathbf{b}\|_1}{\|\mathbf{A}^+(\mathbf{A}\mathbf{x}^{(k)} - \mathbf{b})\|_1} \right) \quad (25)$$

The hyperparameter $0 < c_3 < 1$ is to tune based on the distribution of \mathbf{x}^* . With an upperbound n (the size of the vector \mathbf{x}^*), we obtain (24). Actually (25) can be mathematically derived by assuming the magnitude of the nonzero entries of \mathbf{x}^* are normally distributed. (The derivation can be found in the supplement.) As $k \rightarrow \infty$, it holds that $e^{(k)} \rightarrow 0$ and $p^{(k)} \rightarrow n$, which means that the operator $\eta_{\theta^{(k)}}^{p^{(k)}}$ is getting close to a hard-thresholding operator. The support selection scheme proposed in LISTA-CPSS [7] also follows such principle but it requires more prior knowledge. Compared to that, formula (24) is much more automatic and self-adaptive.

Switching to Conjugate Gradients Theorem 2 suggests that one may call conjugate gradient (CG) to obtain faster convergence as the recovery signal $\mathbf{x}^{(k)}$ is accurate enough. In practice, we choose to switch to CG as k is large enough such that $p^{(k)}$ is large enough. The linear system (20) to be solved by CG depends on the support of \mathbf{x}^* and we estimate the support by the support of $\mathbf{x}^{(k)}$ since we assume $\mathbf{x}^{(k)}$ is accurate enough when we call CG. Finally, HyperLISTA is described in Algorithm 1.

3.5 Hyperparameter-Tuning Options for HyperLISTA

HyperLISTA has reduced the complexity of the learnable parameters to nearly the extreme: only three. While backpropagation remains to be a viable option to solve them, it becomes an over-kill to solve just three variables by passing gradients through tens of neural network layers. Besides, the hyperparameter c_3 in (23) decides the ratio of elements that will be selected into the support and hence passes the thresholding function; that makes c_3 non-differentiable in the computation graph.

Instead, we are allowed to seek simpler, even gradient-free methods to search for the parameters. We also empirically find HyperLISTA has certain robustness to perturbing the found values of c_1, c_2, c_3 , which also encourages us to go with less precise yet much cheaper search methods.

Algorithm 1: HyperLISTA with tuned c_1, c_2, c_3

Input: Observation \mathbf{b} , dictionary \mathbf{A}
1 , hyperparameters c_1, c_2, c_3 . **Initialize :** Let $\mathbf{x}^{(0)} = \mathbf{0}$.
2 Calculate \mathbf{D} and \mathbf{G} with (10), set $\mathbf{W} = (\mathbf{G}^T \mathbf{G}) \mathbf{A}$.
3 Calculate μ with $\mu = \max_{i \neq j} |(\mathbf{D}^T \mathbf{D})_{i,j}|$.
4 **for** $j = 0, 1, 2, \dots$ *until convergence* **do**
5 Conduct iteration (12) with parameters defined in (22 - 24).
6 **if** $p^{(k)}$ *is large enough* **then**
7 **break**
8 **end**
9 **end**
10 Set $S = \text{supp}(\mathbf{x}^{(k)})$, call the conjugate gradient algorithm to solve linear system (20).
Output: $\hat{\mathbf{x}}$, the result of the conjugate gradient.

In this work, we try replacing the backpropagation-based training with the vanilla grid search for learning HyperLISTA. Besides the ultra-light parameterization, another enabling factor is the low evaluation cost on fitness of hyperparameters: just running inference on one minibatch of training samples with them, and no gradient-based training needed. From another aspect, HyperLISTA can be viewed as an iterative algorithm instead of an unfolded neural network. It can be optimized directly on the unseen test data, as long as one wants to afford the cost of re-searching hyperparameters on each dataset, whose cost is still much lower than training using back-propagation.

Specifically, we first use a coarse grid to find an “interested region” of hyperparameters, and then zoom-in with a fine-grained grid. Details are to be found in Section 4.2, and we plan to try other options such as bayesian optimization [12] in future work.

4 Numerical experiments

Experiment settings We use synthesized datasets of 51,200 samples for training, 2,048 validation and 2,048 testing. We follow previous works [7, 18] to use a problem size of $(m, n) = (250, 500)$. The elements in the dictionary \mathbf{A} are sampled from i.i.d. standard Gaussian distribution and we then normalize \mathbf{A} to have unit ℓ_2 column norms. The sparse vectors \mathbf{x}^* are sampled from $N(0, \sigma^2) \cdot \text{Bern}(p)$, where $N(\mu, \sigma^2)$ represents the normal distribution and $\text{Bern}(p)$ the Bernoulli distribution with probability p to take value 1. By default, we choose $\sigma = 1$ and $p = 0.1$, meaning that around 10% of the elements are non-zero whose magnitudes further follows a standard Gaussian distribution. The additive noise ε in (1) follows Gaussian distribution $N(0, \sigma_\varepsilon^2)$. The noise level is measured by signal-to-noise ratio (SNR) in decibel unit. Note that we can change the values of σ , p and σ_ε during testing to evaluate the adaptivity of models. In all experiments, the model performance is measured by normalized mean squared error (NMSE, same as defined in [7, 18]) in decibel unit. All models are unrolled and truncated to 16 layers for training and testing following the typical setting in [7, 18, 31], unless otherwise specified. Besides synthesized data, we also evaluate HyperLISTA on a compressive sensing task using natural images. The results are presented in Appendix B due to limited space.

Comparison Methods: In this section, we compare with the original *LISTA* [15] formulated in (2), *ALISTA* formulated in (4) and its variant with momentum acceleration denoted as *ALISTA-MM* (12). A suffix *-Symm* will be added if a model adopts the symmetric parameterization introduced in Section 3.1. We use *HyperLISTA(-Full)* to represent our proposed method in which we optimize all three hyperparameters c_1, c_2, c_3 in (22) - (24) using grid search. In contrast, we can use back-propagation to train c_1 and c_2 and leave $p^{(k)}$ manually selected as in *ALISTA* because the loss function is not differentiable with respect to $p^{(k)}$. The resulting model is denoted as *HyperLISTA-BP*. Other baselines include *Ada-LISTA* [1] and *NA-ALISTA* [4].

4.1 Validation of symmetric matrix parameterization and Theorem 1

We first validate the efficacy of the symmetric matrix parameterization and Theorem 1, showing the acceleration brought by the momentum term. For this validation, we compare four models: *ALISTA*,

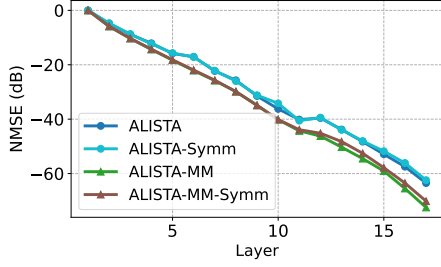


Figure 3: Effect of symmetric matrix parameterization and momentum. Momentum provides acceleration for either parameterization.

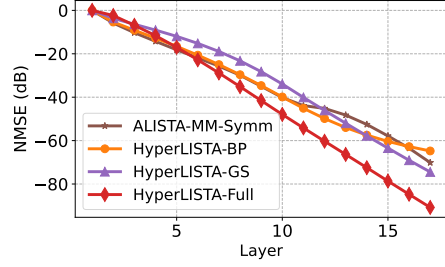
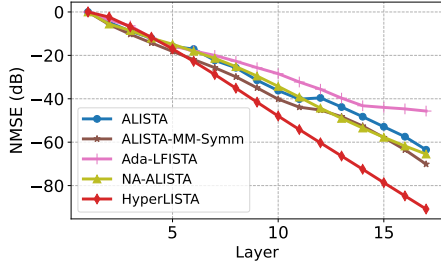
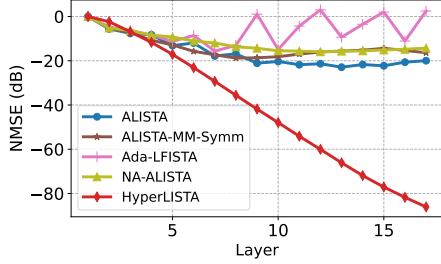


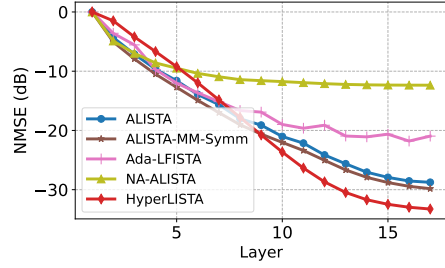
Figure 4: Back-propagation and grid search based training, compared with HyperLISTA-Full with c_1, c_2, c_3 searched.



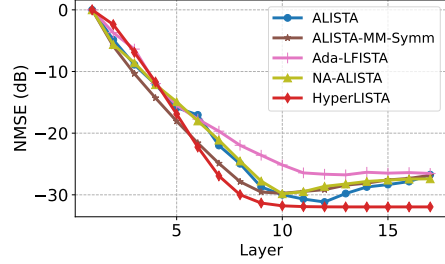
(a) Noiseless. No train/test mismatch.



(c) Variance σ of non-zero elements changed to 2.



(b) Sparsity ratio p changed to 0.15.



(d) Noise level changed to SNR=30dB.

Figure 5: Adaptivity experiments. All models are trained in the noiseless case with $p = 0.1, \sigma = 1.0$, shown in subfigure (a). We directly apply the models trained in (a) to three different settings, which changes p to 0.15, σ to 2 and SNR of the noises to 30 respectively, shown in subfigures (b), (c), (d).

ALISTA-Symm, ALISTA-MM and ALISTA-MM-Symm. We train them on the same dataset and compare their performance measured by NMSE on the testing set. Here, the support selection ratios are selected by following the recommendation in the official implementation of [18]. Results are shown in Figure 3³. As we can see from Figure 3, the symmetric matrix parameterization results in almost no performance drop, corroborating the validity of the new parameterization. On the other hand, introducing momentum to both parameterization brings significant improvement in NMSE.

4.2 Validation of instance-optimal parameter selection and grid search

In this subsection, we show that the adaptive parameterization in Eqns (22) - (24), i.e., HyperLISTA, can perform as well as or even better than the uniform parameterization in (12), and we also show the efficacy of the grid search method. We optimize HyperLISTA-Full using grid search and train HyperLISTA-BP with backpropagation-based method (SGD), respectively. For a fair comparison with HyperLISTA-BP, we introduce a variant of HyperLISTA-Full in which we only grid-search c_1

³Here ALISTA achieves a worse NMSE than that in [18]. We attribute this to the finite-size training set that we use here instead of unlimited training set in [18].

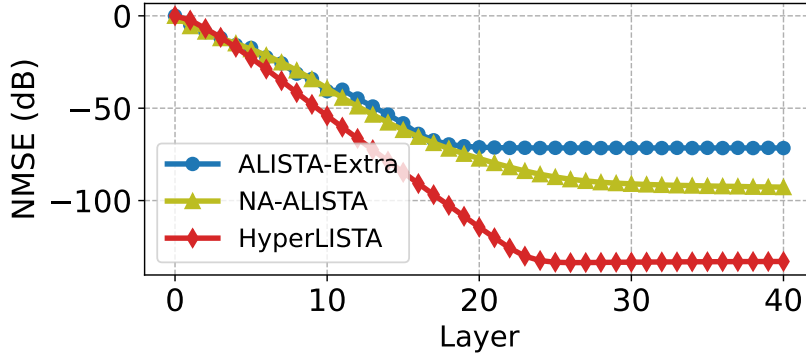


Figure 6: Direct unrolling to 40 layers (all models are trained with 16 layers).

and c_2 in (22) and (23) and use the same $p^{(k)}$ as manually selected in HyperLISTA-BP. We denote this variant as *HyperLISTA-GS*. Figure 4 show that grid search can find even better solutions than backpropagation and the uniform parameterization. When we further use grid search for searching c_1, c_2, c_3 simultaneously (HyperLISTA-Full), there is more performance boost.

4.3 Comparison of adaptivity with previous work

We conduct experiments when there exists mismatch between the training and testing. We instantiate training/testing mismatch in terms of different sparsity levels in the sparse vectors x^* , different distributions of non-zero elements in x^* , and different additive noise levels. We compare HyperLISTA with ALISTA [18] and its variant ALISTA-MM-Symm, Ada-LFISTA [1] and NA-ALISTA [4] which also dynamically generates parameters per input using an external LSTM. Figure 5 show that in the original and all three mismatched cases, HyperLISTA achieves the best performance, especially showing excellent robustness to the non-zero magnitude distribution change (Fig. 5c). Note our computational overhead is also much lower than using LSTM.

Directly unrolling HyperLISTA to more layers Another hidden gem in HyperLISTA is that it learns iteration-independent hyperparameters, which, once searched and trained (on some fixed layer number), can be naturally extended to an arbitrary number of layers. Although NA-ALISTA [4] can also be applied to any number of layers, it has worse performance and adaptivity compared to HyperLISTA, as we compare in Figure 6.

We also compare HyperLISTA with another baseline of 40-layer ALISTA (named as *ALISTA-Extra*), which is directly extrapolated from a 16-layer ALISTA model by reusing the last layer parameters. We can clearly observe that ALISTA cannot directly scale with more layers unrolled.

5 Conclusions and Discussions of Broad Impact

In this paper, we propose a ultra-light weight unrolling network, *HyperLISTA*, for solving sparse linear inverse problems. We first introduce a new ALISTA parameterization and augment it with momentum, and then propose an adaptive parameterization which reduces the training of HyperLISTA to only tuning three **instance- and layer-invariant** hyperparameters. HyperLISTA is theoretically proved and also empirically observed to have super-linear convergence rate as it uses instance-optimal parameters. Compared to previous work, HyperLISTA achieves faster convergence on the seen distribution (i.e., the training data distribution) and shows better adaptivity on unseen distributions.

As a limitation, we do not consider perturbations in dictionaries in this work yet. We also find that HyperLISTA, as a compact model similar to ALISTA [18], may fail to perform well on signals with complicated structures such as real images, where the underlying sparse linear model (1) becomes oversimplified and no longer holds well. We will investigate these further in the future.

We do not see that this work will impose any social risks to the society. Besides the intellectual merits, the largest potential societal impact of this work is that unrolling models can be trained more efficiently and meanwhile more adaptive, increasing the reusability.

References

- [1] Aviad Aberdam, Alona Golts, and Michael Elad. Ada-lista: Learned solvers adaptive to varying models. *arXiv preprint arXiv:2001.08456*, 2020.
- [2] Pierre Ablin, Thomas Moreau, Mathurin Massias, and Alexandre Gramfort. Learning step sizes for unfolded sparse coding. In *Advances in Neural Information Processing Systems*, pages 13100–13110, 2019.
- [3] Amir Beck and Marc Teboulle. A fast iterative shrinkage-thresholding algorithm for linear inverse problems. *SIAM journal on imaging sciences*, 2(1):183–202, 2009.
- [4] Freya Behrens, Jonathan Sauder, and Peter Jung. Neurally augmented ALISTA. In *International Conference on Learning Representations*, 2021.
- [5] HanQin Cai, Jialin Liu, and Wotao Yin. Learned robust pca: A scalable deep unfolding approach for high-dimensional outlier detection. *arXiv preprint arXiv:2110.05649*, 2021.
- [6] Tianlong Chen, Xiaohan Chen, Wuyang Chen, Howard Heaton, Jialin Liu, Zhangyang Wang, and Wotao Yin. Learning to optimize: A primer and a benchmark. *arXiv preprint arXiv:2103.12828*, 2021.
- [7] Xiaohan Chen, Jialin Liu, Zhangyang Wang, and Wotao Yin. Theoretical linear convergence of unfolded ISTA and its practical weights and thresholds. In *Advances in Neural Information Processing Systems*, pages 9079–9089, 2018.
- [8] Benjamin Cowen, Apoorva Nandini Saridena, and Anna Choromanska. Lsalsa: accelerated source separation via learned sparse coding. *Machine Learning*, 108(8-9):1307–1327, 2019.
- [9] Ingrid Daubechies, Michel Defrise, and Christine De Mol. An iterative thresholding algorithm for linear inverse problems with a sparsity constraint. *Communications on Pure and Applied Mathematics: A Journal Issued by the Courant Institute of Mathematical Sciences*, 57(11):1413–1457, 2004.
- [10] David L Donoho, Michael Elad, and Vladimir N Temlyakov. Stable recovery of sparse overcomplete representations in the presence of noise. *IEEE Transactions on information theory*, 52(1):6–18, 2005.
- [11] David L Donoho, Xiaoming Huo, et al. Uncertainty principles and ideal atomic decomposition. *IEEE transactions on information theory*, 47(7):2845–2862, 2001.
- [12] Matthias Feurer and Frank Hutter. Hyperparameter optimization. In *Automated Machine Learning*, pages 3–33. Springer, Cham, 2019.
- [13] Raja Giryes, Yonina C. Eldar, Alex M. Bronstein, and Guillermo Sapiro. Tradeoffs between convergence speed and reconstruction accuracy in inverse problems. *IEEE Transactions on Signal Processing*, 66(7):1676–1690, Apr 2018.
- [14] Gene H Golub and Charles F Van Loan. *Matrix computations*, volume 3. JHU press, 2013.
- [15] Karol Gregor and Yann LeCun. Learning fast approximations of sparse coding. In *Proceedings of the 27th international conference on international conference on machine learning*, pages 399–406, 2010.
- [16] Satoshi Hara, Weichih Chen, Takashi Washio, Tetsuichi Wazawa, and Takeharu Nagai. Spod-net: Fast recovery of microscopic images using learned ista. In *Asian Conference on Machine Learning*, page 694–709, Oct 2019.
- [17] Kuldeep Kulkarni, Suhas Lohit, Pavan Turaga, Ronan Kerviche, and Amit Ashok. Reconnet: Non-iterative reconstruction of images from compressively sensed measurements. In *Proceedings of the IEEE Conference on Computer Vision and Pattern Recognition*, pages 449–458, 2016.
- [18] Jialin Liu, Xiaohan Chen, Zhangyang Wang, and Wotao Yin. Alista: Analytic weights are as good as learned weights in lista. In *International Conference on Learning Representations (ICLR)*, 2019.
- [19] Canyi Lu, Huan Li, and Zhouchen Lin. Optimized projections for compressed sensing via direct mutual coherence minimization. *Signal Processing*, 151:45–55, 2018.
- [20] David Martin, Charless Fowlkes, Doron Tal, and Jitendra Malik. A database of human segmented natural images and its application to evaluating segmentation algorithms and measuring ecological statistics. In *Proceedings Eighth IEEE International Conference on Computer Vision. ICCV 2001*, volume 2, pages 416–423. IEEE, 2001.
- [21] Tianjian Meng, Xiaohan Chen, Yifan Jiang, and Zhangyang Wang. A design space study for lista and beyond. In *International Conference on Learning Representations*, 2021.
- [22] Vishal Monga, Yuelong Li, and Yonina C Eldar. Algorithm unrolling: Interpretable, efficient deep learning for signal and image processing. *arXiv preprint arXiv:1912.10557*, 2019.
- [23] Thomas Moreau and Joan Bruna. Understanding trainable sparse coding with matrix factorization. In *International Conference on Learning Representations*, 2017.

- [24] Yurii E Nesterov. A method for solving the convex programming problem with convergence rate $o(1/k^2)$. In *Dokl. akad. nauk Sssr*, volume 269, pages 543–547, 1983.
- [25] Gregory Ongie, Ajil Jalal, Christopher A Metzler, Richard G Baraniuk, Alexandros G Dimakis, and Rebecca Willett. Deep learning techniques for inverse problems in imaging. *IEEE Journal on Selected Areas in Information Theory*, 1(1):39–56, 2020.
- [26] Dimitris Perdios, Adrien Besson, Philippe Rossinelli, and Jean-Philippe Thiran. Learning the weight matrix for sparsity averaging in compressive imaging. In *2017 IEEE International Conference on Image Processing (ICIP)*, pages 3056–3060. IEEE, 2017.
- [27] Boris T Polyak. Some methods of speeding up the convergence of iteration methods. *Ussr computational mathematics and mathematical physics*, 4(5):1–17, 1964.
- [28] Pablo Sprechmann, Roei Litman, Tal Ben Yakar, Alexander M Bronstein, and Guillermo Sapiro. Supervised sparse analysis and synthesis operators. *Advances in Neural Information Processing Systems*, 26:908–916, 2013.
- [29] Robert Tibshirani. Regression shrinkage and selection via the lasso. *Journal of the Royal Statistical Society: Series B (Methodological)*, 58(1):267–288, 1996.
- [30] Zhangyang Wang, Qing Ling, and Thomas Huang. Learning deep ℓ_0 encoders. In *Proceedings of the AAAI Conference on Artificial Intelligence*, volume 30, 2016.
- [31] Kailun Wu, Yiwen Guo, Ziang Li, and Changshui Zhang. Sparse coding with gated learned ista. In *International Conference on Learning Representations*, 2020.
- [32] Jinxi Xiang, Yonggui Dong, and Yunjie Yang. Fista-net: Learning a fast iterative shrinkage thresholding network for inverse problems in imaging. *IEEE Transactions on Medical Imaging*, 40(5):1329–1339, 2021.
- [33] Bo Xin, Yizhou Wang, Wen Gao, David Wipf, and Baoyuan Wang. Maximal sparsity with deep networks? *Advances in Neural Information Processing Systems*, 29:4340–4348, 2016.
- [34] Yangyang Xu and Wotao Yin. A fast patch-dictionary method for whole image recovery. *Inverse Problems and Imaging*, 10(2):563–583, 2016.
- [35] Chengzhu Yang, Yuantao Gu, Badong Chen, Hongbing Ma, and Hing Cheung So. Learning proximal operator methods for nonconvex sparse recovery with theoretical guarantee. *IEEE Transactions on Signal Processing*, 68:5244–5259, 2020.
- [36] Joey Tianyi Zhou, Kai Di, Jiawei Du, Xi Peng, Hao Yang, Sinno Jialin Pan, Ivor W Tsang, Yong Liu, Zheng Qin, and Rick Siow Mong Goh. Sc2net: Sparse lstms for sparse coding. In *AAAI*, pages 4588–4595, 2018.
- [37] Li Ziang, Wu Kailun, Yiwen Guo, and Changshui Zhang. Learned ista with error-based thresholding for adaptive sparse coding, 2021.

A Empirical Observations on Superlinear Convergence

In this section, we empirically verify the superlinear convergence of HyperLISTA with the switch to conjugate gradient iterations. We apply HyperLISTA to problems with a smaller size: $m = 50, n = 100$. The non-zero elements in the sparse vectors take value 1, instead of following Gaussian distribution in previous experiments. Specifically, we discard support selection in this experiment. Note that setting $c_3 = 0$ in Equation (6), which corresponds to HyperLISTA without support selection, is also in the search space and hence a reasonable option. In this case, we switch to conjugate gradient iterations when the recovered sparse vectors converge to fixed supports for 10 iterations and stop the algorithm as the error is smaller than -250 dB. The supports are estimated by filtering the non-zero elements in the recovered vectors that are smaller than 10% of the maximal magnitudes.

In a single sample testing case shown in Figure 7, the algorithm switches to conjugate gradient iterations after the 12th layer and hence we see an accelerated convergence afterwards. This superlinear convergence rate is also observable on a set of 100 testing samples as shown in Figure 8.

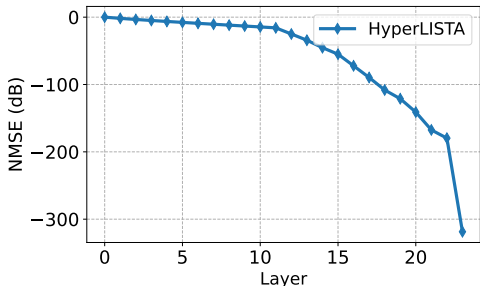


Figure 7: Convergence of HyperLISTA on a single sample.

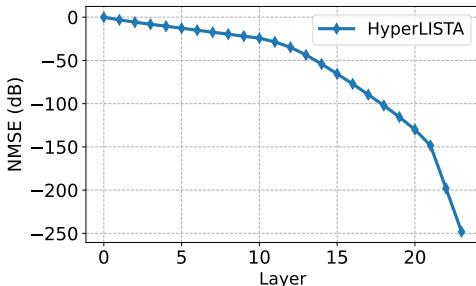


Figure 8: Convergence of HyperLISTA on 100 testing samples.

B Compressive Sensing Experiments on Natural Images

In this section, we conduct a set of compressive sensing experiments on natural images, following a similar setting in [7]. We randomly extract 16x16 patches (flatten into 256-dim vectors then) from the BSD500 dataset [20] to form a training set of 51,200 patches, a validation and a test set of 2,048 patches respectively.

We compressively measure the image signals (256-dim vectors) using a random Gaussian matrix $\Phi \in \mathbb{R}^{128 \times 256}$. We do not add measuring noises. We apply a dictionary learning algorithm in [34] to the training patches of BSD to learn a matrix $T \in \mathbb{R}^{256 \times 512}$, where we assume any patch in a natural image can be represented by a sparse combination of the columns in T . We then use $A = \Phi T$ as the dictionary A in (1). In summary, we denote the image patch as f . The measurement we observe, which is also the input to the network, is generated by $b = \Phi f$. We assume that there exists a sparse vector x^* that satisfies $f \approx T x^*$ and hence $b \approx A x^* = \Phi T x^*$. We apply different methods to recover x^* from measurement b and then reconstruct the image patch by multiplying the recovered sparse vector with T .

Because we do not have access to the underlying ground truth x^* in this real-world scenario, we instead use the LASSO objective function as the loss function for training (of LISTA/ALISTA) or searching (of HyperLISTA), i.e.,

$$Loss = \mathbb{E} \left[\frac{1}{2} \|b - A\hat{x}(b)\|_2^2 + \lambda \|\hat{x}(b)\|_1 \right], \quad (26)$$

where $\hat{x}(b)$ is the sparse vector recovered from the measurement b and λ is the sparsity regularization coefficient. We set $\lambda = 0.05$ in the experiment. We then reconstruct the image signal by $\hat{f} = T\hat{x}$.

We train LISTA and ALISTA [18], and perform grid search to find optimal hyperparameters in HyperLISTA. These three models all have 16 layers. The model performance is evaluated by the average PSNR of the reconstructed images on the standard testing images in Set 11 used in Recon-Net



Figure 9: We visually present the recovered images using 1,000 iterations of FISTA and 16-layer ALISTA and HyperLISTA. We can see that HyperLISTA has much less artifacts at the boundaries of patches.

Method	FISTA 16 iters	FISTA 1,000 iters	LISTA	Recon-Net	ALISTA	HyperLISTA
PSNR (dB)	29.87	30.92	30.85	31.39	32.24	33.46

[17]. The results are shown in the table below, where we also compare with FISTA and Recon-Net. HyperLISTA outperforms other baselines by clear margins. Note that the performance of LISTA is lower than that reported in [7] where 4,000,000 patches are used for training, while we only use 51,200 training patches. We provide visual results of the recovered images in Figure 9, where we can also see HyperLISTA has less patching artifacts compared to ALISTA and FISTA.

C Numerical Algorithm to Calculate Symmetric Dictionary

In this section, we describe how we solve the optimization problem (10):

$$\min_{\mathbf{G}, \mathbf{D}} \|\mathbf{D}^T \mathbf{D} - \mathbf{I}\|_F^2 + \frac{1}{\alpha} \|\mathbf{D} - \mathbf{G}\mathbf{A}\|_F^2, \quad \text{s.t. } \text{diag}(\mathbf{D}^T \mathbf{D}) = \mathbf{1}.$$

Inspired by [19], we use an alternative update algorithm to solve the above problem. Specifically, we first fix \mathbf{G} and update \mathbf{D} with projected gradient descent (PGD):

$$\mathbf{D} \leftarrow \mathcal{P} \left(\mathbf{D} - \zeta \mathbf{D} (\mathbf{D}^T \mathbf{D} - \mathbf{I}) - \frac{\zeta}{\alpha} (\mathbf{D} - \mathbf{G}\mathbf{A}) \right), \quad (27)$$

where \mathcal{P} is the projection operator on the constraint $\text{diag}(\mathbf{D}^T \mathbf{D}) = \mathbf{1}$: normalizing each column of \mathbf{D} . Scalar $\zeta > 0$ is the step size. Secondly, we fix \mathbf{D} and calculate the minimizer of \mathbf{G} with closed-form solution:

$$\mathbf{G} \leftarrow \mathbf{D}\mathbf{A}^+, \quad (28)$$

Directly using such alternative update algorithm is usually slow when α is small since the condition number is large. However, if we choose α as a large number, the difference between \mathbf{D} and $\mathbf{G}\mathbf{A}$ is not enough penalized. Thus, we use first set α as a large number and solve (10) with (27) and (28). As long as we detect convergence, we tune α as a smaller number. Repeat the procedure until $\mathbf{D} \approx \mathbf{G}\mathbf{A}$. The whole algorithm is described in Algorithm 2.

Algorithm 2: Dictionary Solver

Input: The original dictionary \mathbf{A} .**Initialize:** $\mathbf{D} = \mathbf{A}$, $\mathbf{G} = \mathbf{I}$. $\zeta = \alpha = 0.1$.

```
1 for  $j = 0, 1, 2, \dots$  until convergence do
2   Update  $\mathbf{D}$  with (27).
3   Update  $\mathbf{G}$  with (28).
4   Calculate  $f_1 = \|\mathbf{D}^T \mathbf{D} - \mathbf{I}\|_F^2$ .
5   Calculate  $f_2 = \|(\mathbf{G}\mathbf{A})^T \mathbf{G}\mathbf{A} - \mathbf{I}\|_F^2$ .
6   if Two consecutive  $f_1$ s are close enough then
7      $\alpha \leftarrow 0.1\alpha$ .
8      $\zeta \leftarrow 0.1\zeta$ .
9     if  $f_1$  and  $f_2$  are close enough then
10      break
11    end
12  end
13 end
```

Output: \mathbf{D}

D Proof of Theorem 1

Proof. At the beginning of the proof, we define some constants depending on μ, s, B, \underline{B} :

$$\bar{\beta} := (1 - \sqrt{1 - 2\mu s + \mu})^2, \quad (29)$$

$$C_0 := \max\left(1, \frac{5(1 + \bar{\beta})}{(4\bar{\beta} - (\bar{\beta} - \mu s + \mu)^2)(2\mu s - \mu)}\right) \sqrt{s}B, \quad (30)$$

$$\tilde{K}_0 := \left\lceil \frac{\log(\underline{B}) - \log(2C_0)}{\log(2\mu s - \mu)} \right\rceil + 1, \quad (31)$$

In the statement of the theorem, we assume “noise level σ small enough.” Here we give the specific condition on σ :

$$\sigma \leq \min\left(\frac{\underline{B}}{2}, \sqrt{s}B(2\mu s - \mu)^{\tilde{K}_0} \frac{1 - 2\mu s + \mu}{2sC_W}\right). \quad (32)$$

Then we define the parameters we choose in the proof:

$$\theta^{(k)} = \mu \sup_{(\mathbf{x}^*, \varepsilon) \in \mathcal{X}(B, \underline{B}, s, \sigma)} \left\{ \|\mathbf{x}^{(k)} - \mathbf{x}^*\|_1 + C_W \sigma \right\}, \quad (33)$$

$$\gamma^{(k)} = 1, \quad (34)$$

$$\beta^{(k)} = \begin{cases} 0, & k \leq \tilde{K}_0 \\ \bar{\beta}, & k > \tilde{K}_0 \end{cases} \quad (35)$$

$$p^{(k)} = \min\left(\frac{k}{\tilde{K}_0} n, n\right), \quad (36)$$

It is easy to check that the conclusion (16) in the theorem is satisfied.

The whole proof scheme consists of several steps: proving no false positives for all k ; proving the conclusion for $k \leq \tilde{K}_0$; and proving the conclusion for $k > \tilde{K}_0$.

Step 1: no false positives. Firstly, we take an $(\mathbf{x}^*, \varepsilon) \in \mathcal{X}(B, \underline{B}, s, \sigma)$. Let $S = \text{support}(\mathbf{x}^*)$. We want to prove by induction that, as long as (33) holds, $x_i^{(k)} = 0, \forall i \notin S, \forall k$ (no false positives). The statement in the theorem gives $\mathbf{x}^{(0)} = \mathbf{0}$. We follow the same proof line with that in [7] and obtain $\mathbf{x}^{(1)} = \mathbf{0}$. Fixing $k \geq 1$, and assuming $x_i^{(t)} = 0, \forall i \notin S, t = 0, 1, 2, \dots, k$, we have

$$\begin{aligned} x_i^{(k+1)} &= \eta_{\theta^{(k)}}^{p^{(k)}} \left(x_i^{(k)} - (\mathbf{W}_{:,i})^T (\mathbf{A}\mathbf{x}^{(k)} - \mathbf{b}) + \beta^{(k)} (x_i^{(k)} - x_i^{(k-1)}) \right) \\ &= \eta_{\theta^{(k)}}^{p^{(k)}} \left(- \sum_{j \in S} (\mathbf{W}_{:,i})^T \mathbf{A}_{:,j} (x_j^{(k)} - x_j^*) + (\mathbf{W}_{:,i})^T \varepsilon \right), \quad \forall i \notin S. \end{aligned}$$

By the definition of μ :

$$\mu = \max_{i \neq j} \left| (\mathbf{D}_{:,i})^T \mathbf{D}_{:,j} \right| = \max_{i \neq j} \left| (\mathbf{D}^T \mathbf{D})_{i,j} \right| = \max_{i \neq j} \left| (\mathbf{W}^T \mathbf{A})_{i,j} \right|, \quad (37)$$

we have

$$\mu \|\mathbf{x}^{(k)} - \mathbf{x}^*\|_1 \geq \left| - \sum_{j \in S} (\mathbf{W}_{:,i})^T \mathbf{A}_{:,j} (x_j^{(k)} - x_j^*) \right|, \quad \forall i \notin S.$$

By the definition of C_W , we have

$$C_W \sigma \geq \max_{1 \leq j \leq m} |W_{j,i}| \cdot \|\varepsilon\|_1 \geq \left| (\mathbf{W}_{:,i})^T \varepsilon \right|, \quad \forall i = 1, \dots, n.$$

Then we can obtain a lower bound for the threshold $\theta^{(k)}$:

$$\theta^{(k)} \geq \mu \|\mathbf{x}^{(k)} - \mathbf{x}^*\|_1 + C_W \sigma \geq \left| - \sum_{j \in S} (\mathbf{W}_{:,i})^T \mathbf{A}_{:,j} (x_j^{(k)} - x_j^*) + (\mathbf{W}_{:,i})^T \varepsilon \right|,$$

which implies $x_i^{(k+1)} = 0, \forall i \notin S$ by the definition of $\eta_{\theta^{(k)}}^{p^{(k)}}$ in (6). By induction, we have

$$x_i^{(k)} = 0, \forall i \notin S, \quad \forall k. \quad (38)$$

Step 2: analysis for $k \leq \tilde{K}_0$. Since $\beta^{(k)} = 0$ as $k \leq \tilde{K}_0$, ALISTA-MM reduces to ALISTA. One can easily follow the proof line of Theorem 3 in [7] to obtain

$$\|\mathbf{x}^{(k)} - \mathbf{x}^*\|_2 \leq sB(2\mu s - \mu)^k + \frac{2sC_W}{1 + \mu - 2\mu s} \sigma$$

Here we introduce a new proof method to obtain a better bound:

$$\|\mathbf{x}^{(k)} - \mathbf{x}^*\|_2 \leq \sqrt{s}B(2\mu s - \mu)^k + \frac{2sC_W}{1 + \mu - 2\mu s} \sigma. \quad (39)$$

To start our proof, we combine ALISTA-Momentum formula (12) and (38) and obtain

$$\mathbf{x}_S^{(k+1)} = \eta_{\theta^{(k)}}^{p^{(k)}} \left(\mathbf{x}_S^{(k)} - (\mathbf{W}_{:,S})^T (\mathbf{A}_{:,S} \mathbf{x}_S^{(k)} - \mathbf{b}) + \beta^{(k)} (\mathbf{x}_S^{(k)} - \mathbf{x}_S^{(k-1)}) \right).$$

With $\mathbf{b} = \mathbf{A}\mathbf{x}^* + \varepsilon$, we have

$$\mathbf{x}_S^{(k+1)} = \eta_{\theta^{(k)}}^{p^{(k)}} \left(\mathbf{x}_S^{(k)} - (\mathbf{W}_{:,S})^T \mathbf{A}_{:,S} (\mathbf{x}_S^{(k)} - \mathbf{x}_S^*) + (\mathbf{W}_{:,S})^T \varepsilon + \beta^{(k)} (\mathbf{x}_S^{(k)} - \mathbf{x}_S^{(k-1)}) \right).$$

To analyze the thresholding operator $\eta_{\theta^{(k)}}^{p^{(k)}}$, we define $\mathbf{v}^{(k)}$ elementwisely as (The set $S^{p^{(k)}}$ is defined in (7).):

$$v_i^{(k)} \begin{cases} \in [-1, 1] & \text{if } i \in S, x_i^{(k+1)} = 0 \\ = \text{sign}(x_i^{(k+1)}) & \text{if } i \in S, x_i^{(k+1)} \neq 0, i \notin S^{p^{(k)}}(\mathbf{x}^{(k+1)}), \\ = 0 & \text{if } i \in S, x_i^{(k+1)} \neq 0, i \in S^{p^{(k)}}(\mathbf{x}^{(k+1)}). \end{cases} \quad (40)$$

Given (40), we have

$$\begin{aligned} \mathbf{x}_S^{(k+1)} &= \mathbf{x}_S^{(k)} - (\mathbf{W}_{:,S})^T \mathbf{A}_{:,S} (\mathbf{x}_S^{(k)} - \mathbf{x}_S^*) + \beta^{(k)} (\mathbf{x}_S^{(k)} - \mathbf{x}_S^{(k-1)}) \\ &\quad + (\mathbf{W}_{:,S})^T \varepsilon - \theta^{(k)} \mathbf{v}^{(k)}, \quad \forall k \geq 1. \end{aligned} \quad (41)$$

Subtracting \mathbf{x}^* from the both sides of (41), we obtain

$$\begin{aligned} \mathbf{x}_S^{(k+1)} - \mathbf{x}_S^* &= \left((1 + \beta^{(k)}) \mathbf{I}_S - (\mathbf{W}_{:,S})^T \mathbf{A}_{:,S} \right) (\mathbf{x}_S^{(k)} - \mathbf{x}_S^*) - \beta^{(k)} (\mathbf{x}_S^{(k-1)} - \mathbf{x}_S^*) \\ &\quad + (\mathbf{W}_{:,S})^T \varepsilon - \theta^{(k)} \mathbf{v}^{(k)}. \end{aligned} \quad (42)$$

The first term of the above line can be bounded by

$$\left\| (\mathbf{W}_{:,S})^T \varepsilon \right\|_2 \leq \left\| (\mathbf{W}_{:,S})^T \varepsilon \right\|_1 \leq \sum_{i \in S} \left| (\mathbf{W}_{:,i})^T \varepsilon \right| \leq sC_W \sigma.$$

To analyze the norm of vector $\mathbf{v}^{(k)}$, we define

$$\begin{aligned} S^{(k)}(\mathbf{x}^*, \varepsilon) &= \left\{ i \mid i \in S, x_i^{(k+1)} \neq 0, i \in S^{p^{(k)}}(\mathbf{x}^{(k+1)}) \right\}, \\ \bar{S}^{(k)}(\mathbf{x}^*, \varepsilon) &= S \setminus S^{(k)}, \end{aligned} \quad (43)$$

where $S^{(k)}$ depends on \mathbf{x}^* and ε because $\mathbf{x}^{(k+1)}$ depends on \mathbf{x}^* and ε . Given this definition, we have

$$\|\mathbf{v}^{(k)}\|_2 \leq \sqrt{|\bar{S}^{(k)}(\mathbf{x}^*, \varepsilon)|}.$$

As $k \leq \tilde{K}_0$, $\beta^{(k)} = 0$ (35), equation (42) implies

$$\|\mathbf{x}_S^{(k+1)} - \mathbf{x}_S^*\|_2 \leq \|\mathbf{I}_S - (\mathbf{W}_{:,S})^T \mathbf{A}_{:,S}\|_2 \|\mathbf{x}_S^{(k)} - \mathbf{x}_S^*\|_2 + sC_W\sigma + \theta^{(k)} \sqrt{|\bar{S}^{(k)}(\mathbf{x}^*, \varepsilon)|}, \quad k \leq \tilde{K}_0.$$

The definition of μ (37) means each off-diagonal element of matrix $\mathbf{W}^T \mathbf{A}$ is no greater than μ . Thus, the sum of all off-diagonal elements of matrix $(\mathbf{W}^T \mathbf{A})_{S,S}$ is no greater than $\mu(|S| - 1)$. The diagonal elements of matrix $\mathbf{I}_S - (\mathbf{W}^T \mathbf{A})_{S,S}$ are actually zeros by the definition of \mathbf{W} in (10). Then Gershgorin circle theorem [14] implies

$$\|\mathbf{I}_S - (\mathbf{W}^T \mathbf{A})_{S,S}\|_2 \leq \mu(|S| - 1) \leq \mu(s - 1). \quad (44)$$

Since $x_i^{(k)} = 0, \forall i \notin S$, we have $\|\mathbf{x}^{(k)} - \mathbf{x}^*\|_2 = \|\mathbf{x}_S^{(k)} - \mathbf{x}_S^*\|_2$ for all k . Taking supremum on both sides of inequality (41) over $(\mathbf{x}^*, \varepsilon) \in \mathcal{X}(B, \underline{B}, s, \sigma)$, we have

$$\begin{aligned} \sup_{(\mathbf{x}^*, \varepsilon) \in \mathcal{X}(B, \underline{B}, s, \sigma)} \|\mathbf{x}^{(k+1)} - \mathbf{x}^*\|_2 &\leq (\mu(s - 1)) \sup_{(\mathbf{x}^*, \varepsilon) \in \mathcal{X}(B, \underline{B}, s, \sigma)} \|\mathbf{x}^{(k)} - \mathbf{x}^*\|_2 + sC_W\sigma \\ &\quad + \theta^{(k)} \sqrt{\sup_{(\mathbf{x}^*, \varepsilon) \in \mathcal{X}(B, \underline{B}, s, \sigma)} |\bar{S}^{(k)}(\mathbf{x}^*, \varepsilon)|}. \end{aligned}$$

Since $\bar{S}^{(k)}$ is a subset of S , it holds that

$$|\bar{S}^{(k)}(\mathbf{x}^*, \varepsilon)| \leq |S| \leq s.$$

By the definition of $\theta^{(k)}$ in (22), it holds that

$$\begin{aligned} \theta^{(k)} &= \sup_{(\mathbf{x}^*, \varepsilon) \in \mathcal{X}(B, \underline{B}, s, \sigma)} \left\{ \mu \|\mathbf{x}^{(k)} - \mathbf{x}^*\|_1 \right\} + C_W\sigma \\ &\leq \sup_{(\mathbf{x}^*, \varepsilon) \in \mathcal{X}(B, \underline{B}, s, \sigma)} \left\{ \mu \sqrt{s} \|\mathbf{x}^{(k)} - \mathbf{x}^*\|_2 \right\} + C_W\sigma \end{aligned}$$

Combining the above inequalities, we get

$$\sup_{\mathbf{x}^* \in \mathcal{X}(B, \underline{B}, s)} \|\mathbf{x}^{(k+1)} - \mathbf{x}^*\|_2 \leq (2\mu s - \mu) \sup_{\mathbf{x}^* \in \mathcal{X}(B, \underline{B}, s)} \|\mathbf{x}^{(k)} - \mathbf{x}^*\|_2 + 2sC_W\sigma.$$

Denoting $e^{(k)} = \sup_{(\mathbf{x}^*, \varepsilon) \in \mathcal{X}(B, \underline{B}, s, \sigma)} \|\mathbf{x}^{(k)} - \mathbf{x}^*\|_2$, applying the above inequality repeatedly as $k = 0, 1, 2, \dots$, we obtain

$$\begin{aligned} e^{(k)} &\leq (2\mu s - \mu)^k e^{(0)} + 2sC_W\sigma \left(\sum_{t=0}^{k-1} (2\mu s - \mu)^t \right) \\ &\leq (2\mu s - \mu)^k e^{(0)} + \frac{2sC_W}{1 + \mu - 2\mu s} \sigma. \end{aligned}$$

Since $\mathbf{x}^{(0)} = \mathbf{0}$, the term $e^{(0)}$ can be bounded by

$$e^{(0)} = \sup_{(\mathbf{x}^*, \varepsilon) \in \mathcal{X}(B, \underline{B}, s, \sigma)} \|\mathbf{x}^*\|_2 \leq \sqrt{s}B \leq C_0.$$

Then we conclude with

$$\|\mathbf{x}^{(k)} - \mathbf{x}^*\|_2 \leq C_0(2\mu s - \mu)^k + \frac{2sC_W}{1 + \mu - 2\mu s} \sigma, \quad \forall k \leq \tilde{K}_0.$$

Step 3: analysis for $k > \tilde{K}_0$.

Define

$$\delta \mathbf{x}_S = \left((\mathbf{W}_{:,S})^T \mathbf{A}_{:,S} \right)^{-1} (\mathbf{W}_{:,S})^T \varepsilon, \quad \bar{\mathbf{x}}_S = \mathbf{x}_S^* + \delta \mathbf{x}_S. \quad (45)$$

It can be proved that

$$\|\delta \mathbf{x}_S\|_2 \leq \frac{1}{1 + \mu - \mu s} \|(\mathbf{W}_{:,S})^T \varepsilon\|_2 \leq \frac{1}{1 + \mu - \mu s} \|(\mathbf{W}_{:,S})^T \varepsilon\|_1 \leq \frac{s C_W}{1 + \mu - \mu s} \sigma. \quad (46)$$

Then (41) can be rewritten as

$$\mathbf{x}_S^{(k+1)} = \mathbf{x}_S^{(k)} - (\mathbf{W}_{:,S})^T \mathbf{A}_{:,S} (\mathbf{x}_S^{(k)} - \bar{\mathbf{x}}_S) + \beta^{(k)} (\mathbf{x}_S^{(k)} - \mathbf{x}_S^{(k-1)}) - \theta^{(k)} \mathbf{v}^{(k)}.$$

Subtracting $\bar{\mathbf{x}}_S$ from both sides of the above formula, we obtain

$$\mathbf{x}_S^{(k+1)} - \bar{\mathbf{x}}_S = \left((1 + \beta^{(k)}) \mathbf{I}_S - (\mathbf{W}_{:,S})^T \mathbf{A}_{:,S} \right) (\mathbf{x}_S^{(k)} - \bar{\mathbf{x}}_S) - \beta^{(k)} (\mathbf{x}_S^{(k-1)} - \bar{\mathbf{x}}_S) - \theta^{(k)} \mathbf{v}^{(k)}.$$

Plug $\beta^{(k)} = \bar{\beta}$ for $k > \tilde{K}_0$ (35) into the above equation. We obtain

$$\underbrace{\begin{bmatrix} \mathbf{x}_S^{(k+1)} - \bar{\mathbf{x}}_S \\ \mathbf{x}_S^{(k)} - \bar{\mathbf{x}}_S \end{bmatrix}}_{\mathbf{z}^{(k)}} = \underbrace{\begin{bmatrix} (1 + \bar{\beta}) \mathbf{I}_S - (\mathbf{W}_{:,S})^T \mathbf{A}_{:,S} & -\bar{\beta} \mathbf{I}_S \\ \mathbf{I}_S & \mathbf{0} \end{bmatrix}}_{\mathbf{M}} \underbrace{\begin{bmatrix} \mathbf{x}_S^{(k)} - \bar{\mathbf{x}}_S \\ \mathbf{x}_S^{(k-1)} - \bar{\mathbf{x}}_S \end{bmatrix}}_{\mathbf{z}^{(k-1)}} - \theta^{(k)} \begin{bmatrix} \mathbf{v}^{(k)} \\ \mathbf{0} \end{bmatrix}. \quad (47)$$

We claim that \mathbf{M} can be decomposed with

$$\mathbf{M} = \mathbf{T} \Lambda_{\mathbf{M}} \mathbf{T}^{-1}, \quad (48)$$

where $\mathbf{T} \in \mathbb{C}^{2|S| \times 2|S|}$ is nonsingular and $\Lambda_{\mathbf{M}} \in \mathbb{C}^{2|S| \times 2|S|}$ is diagonal and they satisfy

$$\begin{aligned} \|\Lambda_{\mathbf{M}}\|_2 &= \sqrt{\bar{\beta}}, \\ \|\mathbf{T}\|_2 &\leq \sqrt{2 + 2\bar{\beta}}, \\ \|\mathbf{T}^{-1}\|_2 &\leq \frac{\sqrt{2 + 2\bar{\beta}}}{2(4\bar{\beta} - (\bar{\beta} - \mu s + \mu)^2)}. \end{aligned} \quad (49)$$

We will prove claims (48) and (49) later in step 4. Note that matrix \mathbf{M} and its decomposition (48) are not uniform for different instances that satisfy Assumption 1, but the upper bounds in (49) are **uniform** for all instances that satisfy $|S| \leq s$ and $s \leq (1 + 1/\mu)/2$. This is why we do not only calculate the spectral norm of \mathbf{M} as the standard heavy-ball momentum proof: we want to get an **uniform** bound for all instances but not a specific bound for each instance.

Since \mathbf{M} is not symmetric, (47) indicates that $\|\mathbf{x}_S^{(k)} - \bar{\mathbf{x}}_S\|_2$ is NOT monotonically decreasing due to the momentum term. Thus, $\mathbf{v}^{(k)} = \mathbf{0}$ cannot imply $\mathbf{v}^{(k+1)} = \mathbf{0}$. We have to estimate the upperbound of $\|\mathbf{x}_S^{(k)} - \bar{\mathbf{x}}_S\|_2$ by **induction**:

- First we prove that $\mathbf{v}^{(k)} = \mathbf{0}$ as $k = \tilde{K}_0$.
- Then we prove that, if we assume $\mathbf{v}^{(t)} = \mathbf{0}$ for all t satisfies $\tilde{K}_0 \leq t \leq k$ ($k > \tilde{K}_0$), we have

$$\|\mathbf{x}_S^{(k+1)} - \bar{\mathbf{x}}_S\|_2 \leq C_0 (2\mu s - \mu)^{\tilde{K}_0} \left(1 - \sqrt{1 - 2\mu s + \mu} \right)^{k+1 - \tilde{K}_0} \text{ and } \mathbf{v}^{(k+1)} = \mathbf{0}.$$

Now we prove the above two points one-by-one.

First we want to show that $\mathbf{v}^{(k)} = \mathbf{0}$ as $k = \tilde{K}_0$. The definition of \tilde{K}_0 (31) implies

$$C_0 (2\mu s - \mu)^{\tilde{K}_0} < B/2.$$

The assumption on σ (32) implies

$$\frac{2s C_W}{1 - 2\mu s + \mu} \sigma \leq B/2.$$

As $k = \tilde{K}_0$, it holds that, for all $i \in S$

$$|x_i^{(k)} - x_i^*| \leq \|\mathbf{x}^{(k)} - \mathbf{x}^*\|_2 \leq C_0(2\mu s - \mu)^k + \frac{2sC_W}{1 - 2\mu s + \mu}\sigma < \underline{B}. \quad (50)$$

Definition of $p^{(k)}$ in (36) implies $p^{(k)} = n$ for $k \geq \tilde{K}_0$. Based on the definition of η operator (6) and (7), we have $S^{p^{(k)}} = \{1, 2, \dots, n\}$ and the operator $\eta_{\theta^{(k)}}^{p^{(k)}}$ is actually a hard thresholding. The above inequality (50), combined with $|x_i^*| \geq \underline{B} > 0$, implies $x_i^{(k)} \neq 0, i \in S$. Since $p^{(k)} = n$, we have $i \in S^{(k)}(\mathbf{x}^*, \varepsilon)$ for all $i \in S$ according to (43). In another word, $\mathbf{v}^{(k)} = \mathbf{0}$ as $k = \tilde{K}_0$.

Second, we assume $\mathbf{v}^{(t)} = \mathbf{0}$ for all $\tilde{K}_0 \leq t \leq k$ and analyze the variables for $k+1$. Equation (47) and the assumption $\mathbf{v}^{(t)} = \mathbf{0}$ and the matrix decomposition (48) lead to

$$\mathbf{T}^{-1}\mathbf{z}^{(t)} = \Lambda_{\mathbf{M}}\mathbf{T}^{-1}\mathbf{z}^{(t-1)}, \quad \tilde{K}_0 \leq t \leq k.$$

Then we have

$$\mathbf{T}^{-1}\mathbf{z}^{(k)} = \left(\Lambda_{\mathbf{M}}\right)^{k+1-\tilde{K}_0}\mathbf{T}^{-1}\mathbf{z}^{(\tilde{K}_0-1)}.$$

Thus, it holds that

$$\|\mathbf{z}^{(k)}\|_2 \leq \|\Lambda_{\mathbf{M}}\|_2^{k+1-\tilde{K}_0}\|\mathbf{T}\|_2\|\mathbf{T}^{-1}\|_2\|\mathbf{z}^{(\tilde{K}_0-1)}\|_2 \leq \frac{(1+\bar{\beta})\|\mathbf{z}^{(\tilde{K}_0-1)}\|_2}{4\bar{\beta} - (\bar{\beta} - \mu s + \mu)^2} \left(\sqrt{\bar{\beta}}\right)^{k+1-\tilde{K}_0}.$$

By (46), (39) and (32), we have

$$\|\mathbf{z}^{(\tilde{K}_0-1)}\|_2 \leq 2\|\mathbf{x}^{(\tilde{K}_0-1)} - \bar{\mathbf{x}}\|_2 \leq 2\|\mathbf{x}^{(\tilde{K}_0-1)} - \mathbf{x}^*\|_2 + 2\|\delta\mathbf{x}_S\|_2 \leq 5\sqrt{s}B(2\mu s - \mu)^{\tilde{K}_0-1}.$$

Consequently,

$$\|\mathbf{x}_S^{(k+1)} - \bar{\mathbf{x}}_S\|_2 \leq \|\mathbf{z}^{(k)}\|_2 \leq C_0(2\mu s - \mu)^{\tilde{K}_0} \left(1 - \sqrt{1 - 2\mu s + \mu}\right)^{k+1-\tilde{K}_0}.$$

The definition of \tilde{K}_0 (31) gives

$$C_0(2\mu s - \mu)^k < \underline{B}/2, \quad \forall k \geq \tilde{K}_0.$$

It's easy to check that the following inequality holds for all $s \leq (1 + 1/\mu)/2$:

$$1 - \sqrt{1 - 2\mu s + \mu} < 2\mu s - \mu.$$

We conclude that

$$|x_i^{(k+1)} - \bar{x}_i| \leq \|\mathbf{x}_S^{(k+1)} - \bar{\mathbf{x}}_S\|_2 \leq C_0(2\mu s - \mu)^{k+1} < \underline{B}/2, \quad \forall i \in S.$$

With similar arguments as (50), we obtain

$$|x_i^{(k+1)} - x_i^*| \leq |x_i^{(k+1)} - \bar{x}_i| + |\delta x_i| < \underline{B}/2 + \underline{B}/2 = \underline{B}, \quad \forall i \in S$$

and then $\mathbf{v}^{(k+1)} = \mathbf{0}$.

The induction proof is finished and we conclude that, for all $k > \tilde{K}_0$,

$$\begin{aligned} \|\mathbf{x}^{(k)} - \mathbf{x}^*\|_2 &\leq \|\mathbf{x}_S^{(k)} - \bar{\mathbf{x}}_S\|_2 + \|\delta\mathbf{x}_S\|_2 \\ &\leq C_0(2\mu s - \mu)^{\tilde{K}_0} \left(1 - \sqrt{1 - 2\mu s + \mu}\right)^{k+1-\tilde{K}_0} + \frac{sC_W}{1 + \mu - \mu s}\sigma. \end{aligned}$$

As long as we prove (48) and (49), we can finish the whole proof. Proofs of (48) and (49) are actually an estimate of the spectrum of matrix \mathbf{M} and given in "Step 4."

Step 4: spectrum analysis for \mathbf{M} . Since $\mathbf{W}^T\mathbf{A}$ is parameterized in a symmetric way (Section 3.1), its submatrix $(\mathbf{W}_{:,S})^T\mathbf{A}_{:,S}$ is a real symmetric matrix and, consequently, it is orthogonal diagonalizable in the real space:

$$(\mathbf{W}_{:,S})^T\mathbf{A}_{:,S} = \mathbf{U}\Lambda\mathbf{U}^T$$

where $\mathbf{U} \in \mathbb{R}^{|S| \times |S|}$ is orthogonal and $\mathbf{\Lambda} \in \mathbb{R}^{|S| \times |S|}$ is diagonal. The matrix $\mathbf{\Lambda}$ is defined as $\mathbf{\Lambda} = \text{diag}(\lambda_1, \lambda_2, \dots, \lambda_{|S|})$ and its elements are singular values of $(\mathbf{W}_{:,S})^T \mathbf{A}_{:,S}$. Thus, it holds that

$$\begin{aligned} \mathbf{M} &= \begin{bmatrix} \mathbf{U}((1 + \bar{\beta})\mathbf{I}_S - \mathbf{\Lambda})\mathbf{U}^T & -\mathbf{U}(\bar{\beta}\mathbf{I}_S)\mathbf{U}^T \\ \mathbf{U}(\mathbf{I}_S)\mathbf{U}^T & \mathbf{0} \end{bmatrix} \\ &= \begin{bmatrix} \mathbf{U} & \mathbf{0} \\ \mathbf{0} & \mathbf{U} \end{bmatrix} \begin{bmatrix} (1 + \bar{\beta})\mathbf{I}_S - \mathbf{\Lambda} & -\bar{\beta}\mathbf{I}_S \\ \mathbf{I}_S & \mathbf{0} \end{bmatrix} \begin{bmatrix} \mathbf{U}^T & \mathbf{0} \\ \mathbf{0} & \mathbf{U}^T \end{bmatrix}. \end{aligned}$$

By properly permuting the index, we obtain

$$\mathbf{M} = \begin{bmatrix} \mathbf{U} & \mathbf{0} \\ \mathbf{0} & \mathbf{U} \end{bmatrix} \mathbf{P} \begin{bmatrix} \mathbf{B}_1 & & & \\ & \mathbf{B}_2 & & \\ & & \dots & \\ & & & \mathbf{B}_{|S|} \end{bmatrix} \mathbf{P}^{-1} \begin{bmatrix} \mathbf{U}^T & \mathbf{0} \\ \mathbf{0} & \mathbf{U}^T \end{bmatrix} \quad (51)$$

where \mathbf{P} is a permutation operator with $\|\mathbf{P}\|_2 = 1$ and the blocks \mathbf{B}_i is defined as

$$\mathbf{B}_i = \begin{bmatrix} 1 + \bar{\beta} - \lambda_i & -\bar{\beta} \\ 1 & 0 \end{bmatrix}, \quad \forall i = 1, 2, \dots, |S|. \quad (52)$$

The two eigenvalues and eigenvectors of \mathbf{B}_i can be calculated explicitly:

$$\begin{aligned} \lambda_{\mathbf{B}_i,1} &= \frac{1}{2}(1 + \bar{\beta} - \lambda_i + \sqrt{(1 + \bar{\beta} - \lambda_i)^2 - 4\bar{\beta}}) \\ \lambda_{\mathbf{B}_i,2} &= \frac{1}{2}(1 + \bar{\beta} - \lambda_i - \sqrt{(1 + \bar{\beta} - \lambda_i)^2 - 4\bar{\beta}}) \\ \mathbf{v}_{\mathbf{B}_i,1} &= \begin{bmatrix} \lambda_{\mathbf{B}_i,1} \\ 1 \end{bmatrix}, \quad \mathbf{v}_{\mathbf{B}_i,2} = \begin{bmatrix} \lambda_{\mathbf{B}_i,2} \\ 1 \end{bmatrix} \end{aligned}$$

Define

$$\delta(\lambda; \bar{\beta}) = (1 + \bar{\beta} - \lambda)^2 - 4\bar{\beta}$$

that is a one dimensional quadratic function for λ . It is convex and its critical point is $\lambda_* = 1 + \bar{\beta}$. It has two zero points $(1 \pm \sqrt{4\bar{\beta}})^2$. According to (44), the eigenvalues of $(\mathbf{W}_{:,S})^T \mathbf{A}_{:,S}$ are bounded within the following interval

$$1 - \mu(s-1) \leq \lambda_i \leq 1 + \mu(s-1), \quad \forall i = 1, 2, \dots, |S|.$$

It's easy to check that the maximum of $\delta(\lambda; \bar{\beta})$ function is taken at the left boundary:

$$\arg \max_{\lambda \in [1 - \mu(s-1), 1 + \mu(s-1)]} \delta(\lambda; \bar{\beta}) = 1 - \mu(s-1).$$

Since it holds that

$$1 - \mu(s-1) > 1 - 2\mu s + \mu = (1 - \sqrt{\bar{\beta}})^2,$$

we obtain

$$\delta(1 - \mu(s-1); \bar{\beta}) < \delta((1 - \sqrt{\bar{\beta}})^2; \bar{\beta}) = 0.$$

Thus,

$$\delta(\lambda_i; \bar{\beta}) < 0, \quad \forall i = 1, 2, \dots, |S|,$$

which implies that eigenvalues of \mathbf{B}_i has nonzero imaginary part and the two eigenvalues are complex conjugate. The magnitudes of the two eigenvalues can be calculated with

$$|\lambda_{\mathbf{B}_i,1}|^2 = |\lambda_{\mathbf{B}_i,2}|^2 = \frac{1}{4} \left((1 + \bar{\beta} - \lambda_i)^2 - (1 + \bar{\beta} - \lambda_i)^2 + 4\bar{\beta} \right) = \bar{\beta}.$$

Define the imaginary part of $\lambda_{\mathbf{B}_i,1}$ and $\lambda_{\mathbf{B}_i,2}$ as $\Delta_i = -\delta(\lambda_i; \bar{\beta})$, that can be lower bounded by

$$\Delta_i \geq 4\bar{\beta} - (\bar{\beta} - \mu s + \mu)^2 > 0.$$

Concatenate the two eigenvectors together: $\mathbf{V}_i = [\mathbf{v}_{\mathbf{B}_i,1}, \mathbf{v}_{\mathbf{B}_i,2}]$ and the two eigenvalues: $\Lambda_{\mathbf{B}_i} =$

$\begin{bmatrix} \lambda_{\mathbf{B}_i,1} & \\ & \lambda_{\mathbf{B}_i,2} \end{bmatrix}$. Then we have

$$\mathbf{B}_i = \mathbf{V}_i \Lambda_{\mathbf{B}_i} (\mathbf{V}_i)^{-1}$$

Upper bounds for $\|\mathbf{V}_i\|_2$ and $\|(\mathbf{V}_i)^{-1}\|_2$:

$$\|\mathbf{V}_i\|_2 = \left\| \begin{bmatrix} \lambda_{\mathbf{B}_i,1} & \lambda_{\mathbf{B}_i,2} \\ 1 & 1 \end{bmatrix} \right\|_2 \leq \sqrt{2 + 2\bar{\beta}}$$

$$\|(\mathbf{V}_i)^{-1}\|_2 \leq \frac{1}{|\lambda_{\mathbf{B}_i,1} - \lambda_{\mathbf{B}_i,2}|} \left\| \begin{bmatrix} 1 & -\lambda_{\mathbf{B}_i,2} \\ -1 & \lambda_{\mathbf{B}_i,1} \end{bmatrix} \right\|_2 \leq \frac{\sqrt{2 + 2\bar{\beta}}}{2(4\bar{\beta} - (\bar{\beta} - \mu s + \mu)^2)}$$

Concatenate the blocks together:

$$\mathbf{B} = \begin{bmatrix} \mathbf{B}_1 & & \\ & \cdots & \\ & & \mathbf{B}_{|S|} \end{bmatrix}, \Lambda_{\mathbf{M}} = \begin{bmatrix} \Lambda_{\mathbf{B}_1} & & \\ & \cdots & \\ & & \Lambda_{\mathbf{B}_{|S|}} \end{bmatrix}, \mathbf{V} = \begin{bmatrix} \mathbf{V}_1 & & \\ & \cdots & \\ & & \mathbf{V}_{|S|} \end{bmatrix}$$

We have

$$\mathbf{M} = \underbrace{\begin{bmatrix} \mathbf{U} & \mathbf{0} \\ \mathbf{0} & \mathbf{U} \end{bmatrix}}_{\mathbf{T}} \mathbf{P} \mathbf{V} \Lambda_{\mathbf{M}} (\mathbf{V})^{-1} \mathbf{P}^{-1} \underbrace{\begin{bmatrix} \mathbf{U}^T & \mathbf{0} \\ \mathbf{0} & \mathbf{U}^T \end{bmatrix}}_{\mathbf{T}^{-1}}$$

and upper bounds for 2-norms of \mathbf{T} and \mathbf{T}^{-1} :

$$\|\mathbf{T}\|_2 \leq \|\mathbf{V}\|_2 \leq \max_{i=1,2,\dots,|S|} \|\mathbf{V}_i\|_2 \leq \sqrt{2 + 2\bar{\beta}},$$

$$\|\mathbf{T}^{-1}\|_2 \leq \|\mathbf{V}^{-1}\|_2 \leq \max_{i=1,2,\dots,|S|} \|(\mathbf{V}_i)^{-1}\|_2 \leq \frac{\sqrt{2 + 2\bar{\beta}}}{2(4\bar{\beta} - (\bar{\beta} - \mu s + \mu)^2)}.$$

Claims (48) and (49) are proved. With the analysis in step 3, we finish the whole proof. \square

E Proof of Theorem 2

To start the proof, we define some constants depending on μ, s, B, \underline{B} :

$$C_1 := \max\left(C_0, \frac{1 + \mu s - \mu}{1 - \mu s + \mu} \sqrt{s} B\right), \quad (53)$$

$$\tilde{K}_1 := \left\lceil \frac{\log(\underline{B}) - \log(2C_1)}{\log(2\mu s - \mu)} \right\rceil + 2, \quad (54)$$

In the statement of the theorem, we assume “noise level σ is small enough.” Here we give the specific condition on σ :

$$\sigma \leq \min\left(\frac{\underline{B}}{2}, \sqrt{s} B (2\mu s - \mu)^{\tilde{K}_1} \frac{1 - 2\mu s + \mu}{2s C_W}\right). \quad (55)$$

Proof. We first define parameters we choose in the proof:

$$\theta^{(k)} = \gamma^{(k)} \left(\mu \|\mathbf{x}^{(k)} - \mathbf{x}^*\|_1 + C_W \sigma \right), \quad (56)$$

$$p^{(k)} = \min\left(\frac{k}{\tilde{K}_0} n, n\right), \quad (57)$$

The other two parameters $\gamma^{(k)}, \beta^{(k)}$ follow (34), (35) respectively as $k \leq \tilde{K}_1$; $\gamma^{(k)}, \beta^{(k)}$ follow the step size and momentum rules in Conjugate Gradient (CG) respectively as $k > \tilde{K}_1$:

$$\begin{aligned} \mathbf{r}^{(k)} &= (\mathbf{W}_{:,S})^T \left(\mathbf{A}_{:,S} \mathbf{x}_S^{(k)} - \mathbf{b} \right) \\ \alpha^{(k)} &= \|\mathbf{r}^{(k)}\|_2^2 / \|\mathbf{r}^{(k-1)}\|_2^2 \\ \mathbf{d}^{(k)} &= \begin{cases} \mathbf{r}^{(k)}, & k = \tilde{K}_1 + 1 \\ \mathbf{r}^{(k)} + \alpha^{(k)} \mathbf{d}^{(k-1)}, & k > \tilde{K}_1 + 1 \end{cases} \\ \gamma^{(k)} &= \|\mathbf{r}^{(k)}\|_2^2 / \left((\mathbf{W}_{:,S} \mathbf{d}^{(k)})^T \mathbf{A}_{:,S} \mathbf{d}^{(k)} \right) \\ \beta^{(k)} &= \begin{cases} 0, & k = \tilde{K}_1 + 1 \\ \alpha^{(k)} \gamma^{(k)} / \gamma^{(k-1)}, & k > \tilde{K}_1 + 1. \end{cases} \end{aligned} \quad (58)$$

As $k \leq \tilde{K}_1$, we follow the same proof line with Theorem 1 and obtain that $\mathbf{x}^{(k)}$ is close enough to \mathbf{x}^* as $k = \tilde{K}_1$ and it enters a small neighborhood of \mathbf{x}^* where $\text{supp}(\mathbf{x}^{(k)}) = \text{supp}(\mathbf{x}^*)$. Moreover, the ‘no false positive’ conclusion also holds with the new instance-adaptive thresholds (56). Consequently, plugging (58) into (12), one can easily check that (12) is equivalent with applying a conjugate gradient (CG) method starting from $k = \tilde{K}_1 + 1$ on the linear system

$$(\mathbf{W}_{:,s})^T (\mathbf{A}_{:,s} \mathbf{x}_S - \mathbf{b}) = \mathbf{0}. \quad (59)$$

We parameterize our system in a symmetric way (Section 3.1): $(\mathbf{W}_{:,s})^T \mathbf{A}_{:,s} = (\mathbf{D}^T \mathbf{D})_{S,S}$. And $(\mathbf{D}^T \mathbf{D})_{S,S}$ is positive definite according to (44) and $s < (1 + 1/\mu)/2$. Thus, the linear system (59) is a symmetric and positive definite system with solution $\bar{\mathbf{x}}_S$. It is well known that the conjugate gradient method on a symmetric and positive definite system has some important properties:

1. $\|\mathbf{x}_S^{(k)} - \bar{\mathbf{x}}_S\|_2$ is not monotone, but $\|\mathbf{D}_{:,s}(\mathbf{x}_S^{(k)} - \bar{\mathbf{x}}_S)\|_2$ is monotonic nonincreasing.
2. $\mathbf{x}_S^{(k)}$ stops at the solution in finite steps.

With the first property, we use the same techniques with those in Step 3 in the proof of Theorem 1 and obtain

$$\|\mathbf{x}_S^{(k)} - \bar{\mathbf{x}}_S\|_2 \leq \frac{1 + \mu s - \mu}{1 - \mu s + \mu} \|\mathbf{x}_S^{(\tilde{K}_1)} - \bar{\mathbf{x}}_S\|_2, \quad \forall k > \tilde{K}_1,$$

and $\mathbf{v}^{(k)} = \mathbf{0}$ for all $k > \tilde{K}_1$. Consequently, $\text{supp}(\mathbf{x}^{(k)}) = \text{supp}(\mathbf{x}^*)$ holds for all $k > \tilde{K}_1$.

The second property indicates that there is a large enough \tilde{K}_2 such that $\mathbf{x}^{(k)} = \bar{\mathbf{x}}_S$ for all $k > \tilde{K}_2$. In another word, there is a sequence $\{\bar{c}^{(k)}\}$ such that

$$\|\mathbf{x}^{(k)} - \bar{\mathbf{x}}_S\|_2 \leq \|\mathbf{x}^{(0)} - \bar{\mathbf{x}}_S\|_2 \prod_{t=0}^k \bar{c}^{(t)}$$

and it holds that

$$\bar{c}^{(k)} = 0, \quad \forall k > \tilde{K}_2.$$

Finally, $\|\mathbf{x}^{(k)} - \mathbf{x}^*\| \leq \|\mathbf{x}^{(k)} - \bar{\mathbf{x}}_S\| + \|\bar{\mathbf{x}}_S - \mathbf{x}^*\|_2$. Combining the above upper bound and (46), we obtain (17). Theorem 2 is proved. \square

F Instance-Adaptive Parameters for ALISTA without Momentum

Actually we can prove that ALISTA without momentum (setting $\beta^{(k)} = 0$ for all k in (12)) also converge superlinearly if the parameters are taken in an instance-adaptive way. We list the theorem bellow and will discuss why we choose ALISTA-momentum rather than ALISTA without momentum following Theorem 3 and its proof.

Theorem 3. *Let $\mathbf{x}^{(0)} = \mathbf{0}$ and $\{\mathbf{x}^{(k)}\}_{k=1}^\infty$ be generated by (12) and set $\beta^{(k)} = 0$ for all k . If Assumption 1 holds and $s < (1 + 1/\mu)/2$ and σ is small enough, then there exists a sequence of parameters $\{\theta^{(k)}, p^{(k)}, \gamma^{(k)}\}_{k=1}^\infty$ for each instance $(\mathbf{x}^*, \varepsilon) \in \mathcal{X}(B, \underline{B}, s, \sigma)$ so that we have:*

$$\|\mathbf{x}^{(k)} - \mathbf{x}^*\|_2 \leq \sqrt{s} B \prod_{t=0}^k \hat{c}^{(t)} + \frac{2sC_W}{1 - 2\mu s + \mu} \sigma, \quad \forall k = 1, 2, \dots, \quad (60)$$

where the convergence rate $\hat{c}^{(k)}$ satisfies

$$\hat{c}^{(k)} \rightarrow 0 \text{ as } k \rightarrow \infty. \quad (61)$$

Proof. Similar with the previous two proofs, we introduce some constants to facilitate the proof.

$$\tilde{K}_3 := \left\lceil \frac{\log(\underline{B}) - \log(2\sqrt{s}B)}{\log(2\mu s - \mu)} \right\rceil + 1. \quad (62)$$

We assume that

$$\sigma \leq \min\left(\frac{B}{2}, \sqrt{s}B(2\mu s - \mu)^{\tilde{K}_3}\right) \frac{1 - 2\mu s + \mu}{2sC_W}. \quad (63)$$

The parameters are taken as

$$\theta^{(k)} = \gamma^{(k)}\left(\mu\|\mathbf{x}^{(k)} - \mathbf{x}^*\|_1 + C_W\sigma\right), \quad \forall k \quad (64)$$

$$p^{(k)} = \min\left(\frac{k}{\tilde{K}_3}n, n\right), \quad \forall k \quad (65)$$

$$\gamma^{(k)} = \begin{cases} 1, & k \leq \tilde{K}_3 \\ 1/\lambda_i, & k = \tilde{K}_3 + i, 1 \leq i \leq |S| \\ \text{any real number,} & k \geq \tilde{K}_3 + |S| \end{cases} \quad (66)$$

where λ_i is the i -th singular value of $(\mathbf{W}_{:,S})^T \mathbf{A}_{:,S}$.

With (62), (63), (64), (65), (66), and following the same proof line as Theorem 1, one can prove that

- No false positive: $x_i^{(k)} = 0$ for all $i \in S$ and $k \geq 0$.
- Linear convergence: $\|\mathbf{x}^{(k)} - \mathbf{x}^*\|_2 \leq \sqrt{s}B(2\mu s - \mu)^k + \frac{2sC_W}{1-2\mu s + \mu}\sigma$ for all $k \leq \tilde{K}_3$.

Since $\beta^{(k)} = 0$, the metric $\|\mathbf{x}^{(k)} - \mathbf{x}^*\|_2$ must be monotone and, consequently, $\mathbf{v}^{(k)} = \mathbf{0}$ for all $k \geq \tilde{K}_3$ because $\mathbf{x}^{(k)}$ will stay in the neighborhood that $\text{supp}(\mathbf{x}^{(k)}) = \text{supp}(\mathbf{x}^*)$ once it enters the neighborhood. Thus, for $k > \tilde{K}_3$, formula (12) reduces to

$$\mathbf{x}_S^{(k+1)} = \mathbf{x}_S^{(k)} - \gamma^{(k)}(\mathbf{W}_{:,S})^T (\mathbf{A}_{:,S}\mathbf{x}_S^{(k)} - \mathbf{b}).$$

Denoting $\mathbf{Q} = (\mathbf{W}_{:,S})^T \mathbf{A}_{:,S}$, plugging in (45), we obtain

$$\begin{aligned} \mathbf{x}_S^{(k+1)} &= \mathbf{x}_S^{(k)} - \gamma^{(k)}\mathbf{Q}(\mathbf{x}_S^{(k)} - \bar{\mathbf{x}}_S) \\ \mathbf{x}_S^{(k+1)} - \bar{\mathbf{x}}_S &= \mathbf{x}_S^{(k)} - \bar{\mathbf{x}}_S - \gamma^{(k)}\mathbf{Q}(\mathbf{x}_S^{(k)} - \bar{\mathbf{x}}_S) \\ \mathbf{x}_S^{(k+1)} - \bar{\mathbf{x}}_S &= (\mathbf{I} - \gamma^{(k)}\mathbf{Q})(\mathbf{x}_S^{(k)} - \bar{\mathbf{x}}_S) \end{aligned}$$

Since \mathbf{Q} is real symmetric, it can be orthogonal diagonalized: $\mathbf{Q} = \mathbf{U}\Sigma\mathbf{U}^T$, where \mathbf{U} is an orthogonal matrix and $\Sigma = \text{diag}(\sigma_1, \sigma_2, \dots, \sigma_n)$. Then,

$$\begin{aligned} \mathbf{x}_S^{(k+1)} - \bar{\mathbf{x}}_S &= (\mathbf{U}\mathbf{U}^T - \gamma^{(k)}\mathbf{U}\Sigma\mathbf{U}^T)(\mathbf{x}_S^{(k)} - \bar{\mathbf{x}}_S) \\ \mathbf{U}^T(\mathbf{x}_S^{(k+1)} - \bar{\mathbf{x}}_S) &= (\mathbf{I} - \gamma^{(k)}\Sigma)\mathbf{U}^T(\mathbf{x}_S^{(k)} - \bar{\mathbf{x}}_S) \end{aligned}$$

Denoting $\mathbf{y}^{(k)} = \mathbf{U}^T(\mathbf{x}_S^{(k)} - \bar{\mathbf{x}}_S)$, we have

$$\begin{aligned} \mathbf{y}^{(k+1)} &= (\mathbf{I} - \gamma^{(k)}\Sigma)\mathbf{y}^{(k)}. \\ y_i^{(k+1)} &= (1 - \gamma^{(k)}\sigma_i)y_i^{(k)}, \quad i = 1, 2, \dots, |S|. \end{aligned}$$

Plugging in the parameters $\gamma^{(k)} = 1/\sigma^i$ for $k = \tilde{K}_3 + i$, we have

$$\begin{aligned} y_1^{(k)} &= 0, \quad \text{as } k \geq \tilde{K}_3 + 2 \\ y_2^{(k)} &= 0, \quad \text{as } k \geq \tilde{K}_3 + 3 \\ &\dots \\ y_{|S|}^{(k)} &= 0, \quad \text{as } k \geq \tilde{K}_3 + |S| + 1 \end{aligned}$$

That is, $\mathbf{y}^{(k)} = \mathbf{0}$ for $k \geq \tilde{K}_3 + |S| + 1$. Consequently, $\mathbf{x}^{(k)} = \bar{\mathbf{x}}$ for $k \geq \tilde{K}_3 + |S| + 1$. This conclusion, combined with (46), implies (60) and (61) and finishes the proof. \square

F.1 Some discussions

Although both ALISTA and ALISTA-momentum achieves superlinear convergence, ALISTA-momentum performs better than ALISTA. To achieve superlinear convergence, ALISTA has to take step size as $\gamma^{(k)} = 1/\lambda_i$ (66) where λ_i is one of the eigenvalues of $\mathbf{W}_{:,S}^T \mathbf{A}_{:,S}$. Such step size rule is not easy to calculate in practice and numerically unstable compared with the conjugate gradient in HyperLISTA. This is why we choose ALISTA-momentum and its instance-adaptive variant: HyperLISTA.

Theorem 3 itself shows that ALISTA with adaptive parameters converges faster than that with uniform parameters over instances. NA-ALISTA [4] learns instance-adaptive parameter rule with LSTMs and shows good numerical performance. Theorem 3 actually provides a theoretical explanation for this approach.

G Derivation of the Support Selection Formula

In this section, we provide the derivation of $p^{(k)}$ formula (24).

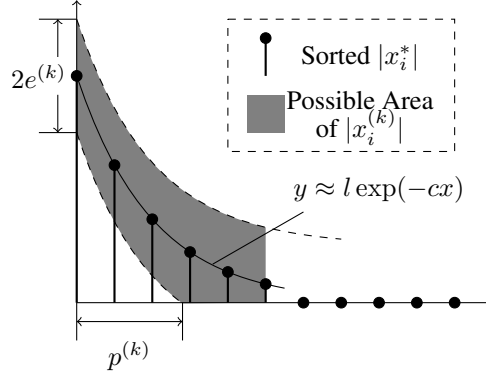


Figure 10: Choice of support selection (with more details)

We put the diagram of support selection (Figure 2) with more details in Figure 10. To estimate $p^{(k)}$, one should make assumptions on the distribution of the magnitudes of x_i^* . We assume that the nonzero entries of \mathbf{x}^* follows normal distribution. The possibility of x_i^* having a large magnitude is smaller than the possibility of x_i^* having a small magnitude. Thus, the curve connecting “sorted $|x_i^*|$ ” in Figure 10 should be a convex function. Here we take exponential function $y = l \exp(-cx)$ to approximate the distribution. The intersection of the curve $y = l \exp(-cx)$ and the y -axis is $l = \max_i(x_i^*)$, i.e., $l = \|\mathbf{x}^*\|_\infty$. The lower bound of the gray area in Figure 10 is a shift of $y = l \exp(-cx)$. Thus, the relationship between $e^{(k)}$, $p^{(k)}$ can be formulated as

$$\|\mathbf{x}^*\|_\infty \exp(-cp^{(k)}) - e^{(k)} = 0.$$

Equivalently,

$$p^{(k)} = \frac{1}{c} \log \left(\frac{\|\mathbf{x}^*\|_\infty}{e^{(k)}} \right) = \frac{1}{c} \log \left(\frac{\|\mathbf{x}^*\|_\infty}{\|\mathbf{x}^{(k)} - \mathbf{x}^*\|_\infty} \right).$$

Constant c depends on the distribution of \mathbf{x}^* . In practice, we use $c_3 = 1/c$ as the hyperparameter to tune. Furthermore, we use $\|\mathbf{A}^+ \mathbf{b}\|_1$ to estimate $\|\mathbf{x}^*\|$ and use residual $\|\mathbf{A}^+ (\mathbf{A} \mathbf{x}^{(k)} - \mathbf{b})\|_1$ to estimate the error $\|\mathbf{x}^{(k)} - \mathbf{x}^*\|$. Then formula (25) is obtained. With an upper bound of n , (24) is obtained.